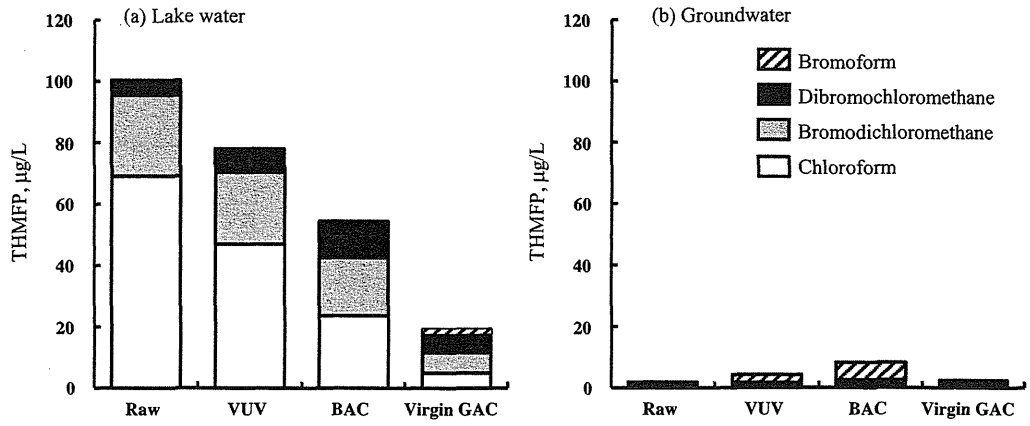

Fig. 6 – Changes in THMFPs in (a) lake water and (b) groundwater with VUV treatment (7.8 kJ/L) and subsequent treatment with BAC or virgin GAC. The values represent averages for two samples (6 measurements).

in the JDWQS (CAA, DCAA, and TCAA; 20, 40, and 200 μg/L, respectively).

Six of the nine HAAs (CAA, DBAA, BCAA, DCAA, TCAA, and BDCAA) were detected in the lake water samples after chlorination, whereas BAA, DBCAA, and TBAA were not detected (Fig. 7(a)). The HAAFP (i.e., the sum of the concentrations of the 9 HAAs after chlorination) of the raw lake water was approximately 80 μg/L. TCAA was present at the highest concentration (45 μg/L), followed by DCAA (23 μg/L). The concentrations of these compounds were under the JDWQS value. However, the HAA_5 value of the chlorinated lake water was 69 μg/L, which exceeded the USEPA regulation value. Unlike THMFP, HAAFP was not decreased by VUV treatment. Malliarou et al. (2005) have reported that the relationship between THMs and HAAs is site specific; in the present study, the precursors of the HAAs may have differed from those of the THMs. Buchanan et al. (2006) reported that HAAFP remains basically constant, with only small fluctuations, upon VUV irradiation at ≤32 J/cm^2 but decreases upon VUV irradiation at ≥48 J/cm^2. Our results at the lower VUV dose roughly agreed with theirs.

Precursors of HAAs in the VUV-treated lake water were effectively removed by the subsequent GAC treatment, reducing HAAFP. Buchanan et al. (2008) reported that HAAFP decreases with BAC treatment. We found that the HAA precursors could also be removed adsorptively even without the activity of microorganisms inhabiting the activated carbon. The BAC and virgin GAC treatments decreased HAAFP to 35 and 13 μg/L (23 and 7 μg/L as HAA_5), respectively, values that meet the USEPA HAA_5 standard. Finally, HAAFP was decreased by the GAC treatment, even though it did not decrease during VUV treatment at the VUV dose used in the present study.

The groundwater used in the present study did not produce any HAAs after chlorination (Fig. 7(b)). As was the case for THMs, the groundwater did not contain HAA precursors. After VUV treatment and subsequent GAC treatment, no HAAFP was observed likewise.

3.4.3. *Aldehydes*

Aldehydes are the main disinfection by-products of ozonation (Cancho et al., 2002), but aldehydes are also reportedly produced by chlorination (Kransner et al., 1989). Formaldehyde has been reported to be mutagenic (Lewis and Chestner, 1981) and is classified as a human carcinogen (Group A) by the International Agency for Research on Cancer. Various other aldehydes have also been reported to be mutagenic (Brambilla et al., 1989); in particular, glyoxal is reportedly more mutagenic than formaldehyde (Marnett et al., 1985). Among the 10 aldehydes measured in the present study, formaldehyde is the only one with regulated values for drinking water: 80 and 900 μg/L in the JDWQS and the WHO guidelines, respectively. In the present study, four of the ten aldehydes (formaldehyde, propanal, butanal, and glyoxal) were detected in the chlorinated samples.

The raw lake water used in the experiments contained no aldehydes (data not shown), whereas after chlorination, the water contained some aldehydes (Fig. 8(a)), which were

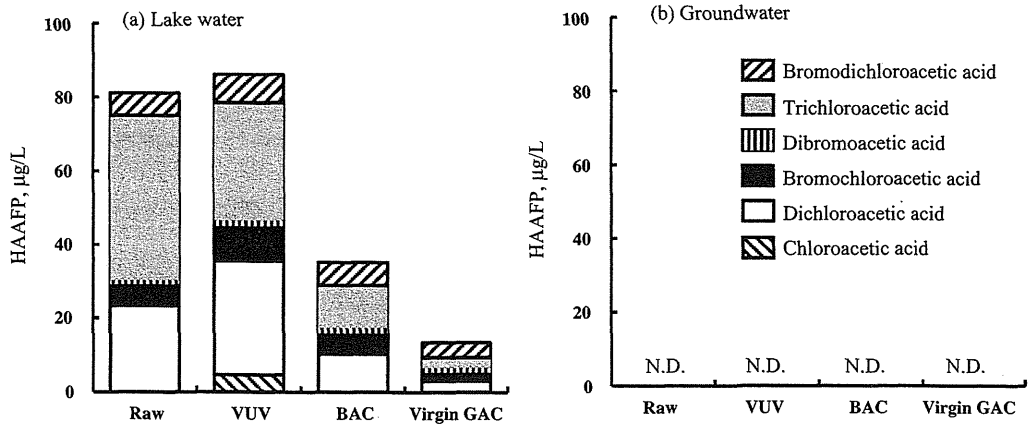

Fig. 7 – Changes in HAAFPs in (a) lake water and (b) groundwater with VUV treatment (7.8 kJ/L) and subsequent treatments with BAC or virgin GAC. The values represent averages for 2 samples (6 measurements).

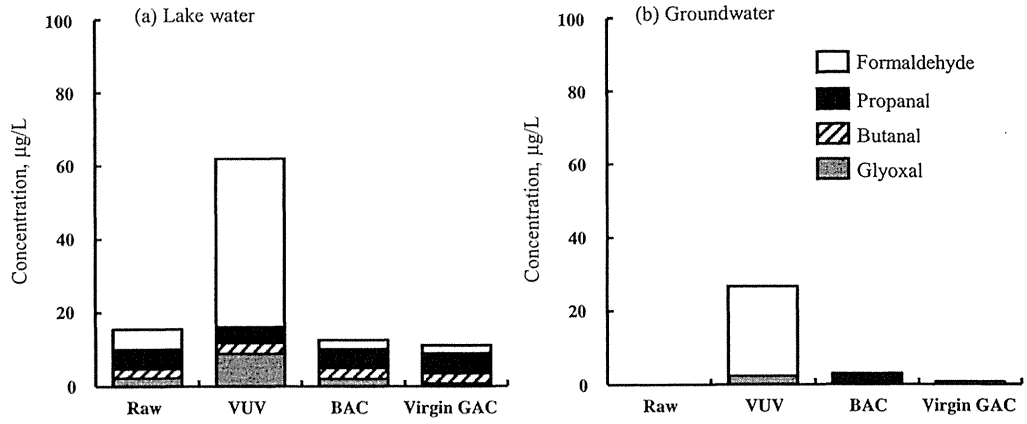

Fig. 8 – Changes in aldehyde concentrations after chlorination of (a) lake water and (b) groundwater with VUV treatment (7.8 kJ/L) and subsequent treatments with BAC or virgin GAC. The values represent averages for two samples (six measurements).

produced by the reaction of chlorine with NOM (Becher et al., 1992) present in the raw water. After VUV treatment followed by Cl_2 treatment (VUV/Cl_2), a relatively high concentration (approximately 40 μg/L) of formaldehyde was observed. Thomson et al. (2004) reported that formaldehyde was the dominant species among low molecular weight carbonyl compounds present in a VUV-irradiated surface water, which agrees with our results. Zhang et al. (2008) reported that aldehydes are produced from NOM during a catalytic ozonation process, in which hydroxyl radicals play a critical role, and that among the aldehydes, formaldehyde was produced in the largest amounts. During VUV treatment in the present study, most of the reactions that occurred were caused by hydroxyl radicals, and this is likely the reason that a large amount of formaldehyde was produced. Additionally, some of the NOM that was not converted to formaldehyde during chlorination may have been transformed to formaldehyde-forming compounds during VUV treatment, and therefore would also contribute to the increase in the formaldehyde concentration after chlorination. Glyoxal was also observed in the lake water subjected to VUV/Cl_2 treatment, and this result agrees with previous results reported by (Zhang et al., 2008). However, when the VUV-treated lake water was subsequently treated with BAC or virgin GAC, the formaldehyde and glyoxal concentrations observed after the final chlorination were substantially lower than before the carbon treatment. This decrease may have been due to biological or adsorptive removal of aldehyde-forming precursors, aldehydes produced by VUV treatment, or both. In summary, aldehydes were produced during VUV treatment but their concentrations could be reduced by subsequent treatment with BAC or GAC. These results clearly indicate that VUV treatment should be used in combination with BAC or GAC treatment for optimum removal of disinfection by-products.

The raw groundwater contained no aldehydes (data not shown), and no aldehydes were detected even after chlorination (Fig. 8(b)), indicating that aldehyde-forming precursors were probably not present in the raw groundwater. However, formaldehyde was observed in the chlorinated VUV-treated groundwater, which indicates that some of the organic matter in the raw groundwater was transformed into either formaldehyde or formaldehyde precursors by VUV treatment. The formaldehyde precursors and formaldehyde itself were effectively removed by both BAC and virgin GAC, in agreement with the results observed with the lake water. Only a small amount of aldehydes was detected after the BAC and GAC treatments.

3.4.4. *Nitrite*

Nitrite is formed by the reaction of nitrate with solvated electrons and hydrogen atoms that are formed by VUV photolysis of water (Zoschke et al., 2014); nitrite formation should be taken into account in real-world applications of VUV irradiation. Nitrite was produced by VUV irradiation of the raw lake water (Fig. 9(a)), but the concentration was very low (0.2 mg-N/L) because the nitrate concentration of the raw lake water was also very low. In contrast, the nitrite concentration produced by VUV irradiation of the raw groundwater was 1.3 mg-N/L (Fig. 9(b)), which exceeds the USEPA maximum contaminant level (1 mg-N/L) and the European drinking water standard (0.1 mg-N/L). The nitrite was not removed by subsequent treatment with virgin GAC. However, subsequent BAC treatment completely removed the nitrite. Nitrifying bacteria in the GAC most likely oxidized the nitrite to nitrate. For nitrite removal, BAC treatment is recommended after VUV irradiation.

3.4.5. *Bromate*

To investigate bromate production from bromide, we prepared buffered DTW spiked with bromide at a high concentration (100 μg-Br/L), and we then conducted decomposition experiments using the VUV, VUV/TiO_2, UV, and UV/TiO_2 treatments (10.8 kJ/L). After all the treatments, the bromate concentrations (<0.1 μg-BrO_3^-/L) were well below the WHO guideline value, the USEPA maximum contaminant level, and the JDWQS value (10 μg-BrO_3^-/L) (data not shown). Several methods for suppressing bromate production during ozonation have been reported (Pinkernell and von Gunten, 2001), but in actual practice, the difficulty in keeping certain operation parameters in a suitable range may limit the application of the ozonation process. In contrast, the VUV, VUV/H_2O_2, and UV/H_2O_2 treatments minimized the formation of bromate even when the raw water was contaminated with a high concentration of bromide.

To minimize by-product formation during VUV treatment, subsequent treatment with GAC or BAC is recommended. The efficiency of 1,4-dioxane decomposition by VUV treatment was lower than the efficiencies by the other AOPs. However, VUV treatment is operationally simple and requires no

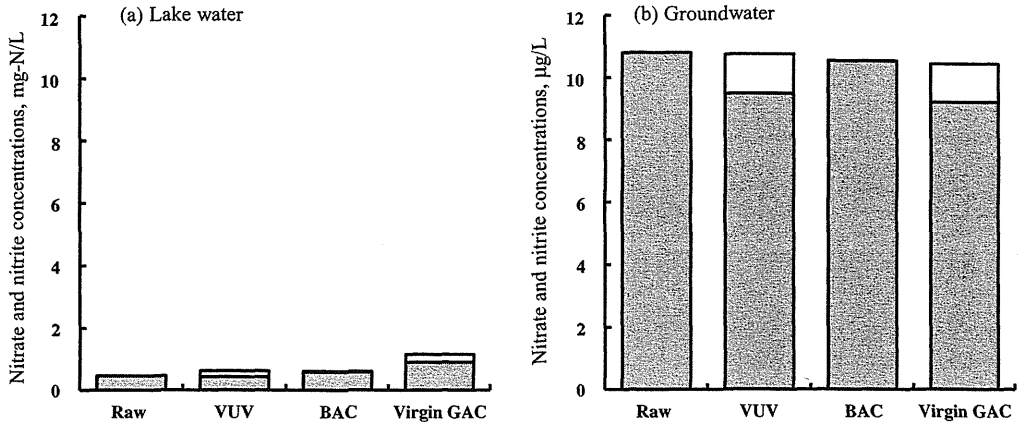

Fig. 9 – Change in nitrate (gray) and nitrite (white) concentrations in (a) lake water and (b) groundwater with VUV treatment (7.8 kJ/L) and subsequent treatments with BAC or virgin GAC. The values represent averages for two samples (six measurements).

chemicals. VUV treatment was revealed to effectively decompose 1,4-dioxane with economic feasibility, and by-product formation could be suppressed by subsequent GAC or BAC treatment. Thomson et al. (2002) reported that the EE/O values for the VUV treatment on NOM removal were approximately 80 (based on OD_{254}) and 200 (based on DOC) kWh/(m^3·order), respectively, and they were still >20 kWh/(m^3·order) even with 50 mg/L of hydrogen peroxide addition. These values were much larger than the values (<1 kWh/(m^3·order)) obtained in the present study for 1,4-dioxane removal, and regarded to be economically infeasible under the EE/O criterion (feasible when EE/O < 10). Accordingly, not NOM but persistent compounds, such as 1,4-dioxane, that are quite difficult to be removed by other treatment methods are recommended to be included in main targets of the VUV treatment.

4. Conclusions

1. For the first time, VUV treatment was used to decompose 1,4,-dioxane, a persistent organic compound, in water, and the treatment was found to be economically feasible. The rate of 1,4-dioxane decomposition for the treatments increased in the order UV < UV/TiO_2 < VUV < VUV/TiO_2. The rate constant for 1,4-dioxane decomposition was smaller than the rate constants for 2-MIB and geosmin decomposition in all of the tested treatments.
2. Addition of H_2O_2 accelerated the decomposition of 1,4-dioxane during both UV and VUV treatments. VUV/H_2O_2 treatment was superior to UV/H_2O_2 treatment at a small H_2O_2 dose, but the decomposition efficiencies of the two treatments were almost the same at a large H_2O_2 dose.
3. VUV treatment slightly decreased THMFP but had no effect on HAAFP, whereas the treatment increased the total aldehyde concentration. However, THMFP, HAAFP, and aldehyde concentration could be reduced by subsequent GAC treatment. Although nitrite was produced during VUV treatment, it completely disappeared after subsequent BAC treatment. VUV treatment should be used in combination with BAC or GAC treatment to minimize by-product formation. Even though the raw water contained a high concentration of bromide (100 μg-Br/L), no bromate (<0.1 μg-BrO_3^-/L) was produced by VUV treatment.
4. The combination of VUV and BAC or GAC treatments is simple and requires no chemicals, and it effectively and economically removed 1,4-dioxane with limited by-product formation.

Acknowledgements

This research was supported in part by a Grant-in-Aid for Scientific Research (S) (24226012), Health and Labor Sciences Research Grant (Research on Health Security Control), and by Bureau of Waterworks, Tokyo Metropolitan Government.

References

Abe, A., 1999. Distribution of 1,4-dioxane in relation to possible sources in the water environment. Sci. Total Environ. 227, 41–47.

Adams, C.D., Scanlan, P.A., Secrist, N.D., 1994. Oxidation and biodegradability enhancement of 1,4-dioxane using hydrogen peroxide and ozone. Environ. Sci. Technol. 28, 1812–1818.

Afzal, A., Oppenländer, T., Bolton, J.R., El-Din, M.G., 2010. Anatoxin-a degradation by advanced oxidation processes: vacuum-UV at 172 nm, photolysis using medium pressure UV and UV/H2O2. Water Res. 44, 278–286.

Andrews, S., Huck, P., Chute, A., Bolton, J., Anderson, W., 1995. UV oxidation for drinking water-feasibility studies for addressing specific water quality issues. AWWA Annu. Conf., 1881–1898.

Becher, G., Ovrum, N.M., Christman, R.F., 1992. Novel chlorination by-products of aquatic humic substances. Sci. Total Environ. 117–118, 509–520.

Black, D.B., Lawrence, R.C., Lovering, B.G., Watson, J.R., 1983. Gas-liquid chromatographic method for determining 1,4-dioxane in cosmetics. J. Assoc. Off. Anal. Chem. 66, 180–183.

Bolton James, R., Bircher Keith, G., Tumas, W., Tolman Chadwick, A., 2001. Figures-of-merit for the technical development and application of advanced oxidation technologies for both electric- and solar-driven systems (IUPAC Technical Report). Pure Appl. Chem., 627.

Brambilla, G., Cajelli, E., Canonero, R., Martelli, A., Marinari, U.M., 1989. Mutagenicity in V79 Chinese hamster cells of n-alkanals produced by lipid peroxidation. Mutagenesis 4, 277–279.

Buchanan, W., Roddick, F., Porter, N., 2006. Formation of hazardous by-products resulting from the irradiation of natural organic matter: comparison between UV and VUV irradiation. Chemosphere 63, 1130–1141.

Buchanan, W., Roddick, F., Porter, N., 2008. Removal of VUV pre-treated natural organic matter by biologically activated carbon columns. Water Res. 42, 3335–3342.

Buchanan, W., Roddick, F., Porter, N., Drikas, M., 2005. Fractionation of UV and VUV pretreated natural organic matter from drinking water. Environ. Sci. Technol. 39, 4647–4654.

Cancho, B., Ventura, F., Galceran, M.T., 2002. Determination of aldehydes in drinking water using pentafluorobenzylhydroxylamine derivatization and solid-phase microextraction. J. Chromatogr. A 943, 1–13.

Cantor, K.P., Lynch, C.F., Hildesheim, M., Dosemeci, M., Lubin, J., Alavanja, M., Craun, G., 1998. Drinking water source and chlorination byproducts I. Risk of bladder cancer. Epidemiology 9, 21–28.

Chang, E.E., Chiang, P.-C., Ko, Y.-W., Lan, W.-H., 2001. Characteristics of organic precursors and their relationship with disinfection by-products. Chemosphere 44, 1231–1236.

Coleman, H.M., Vimonses, V., Leslie, G., Amal, R., 2007. Degradation of 1,4-dioxane in water using TiO_2 based photocatalytic and H2O2/UV processes. J. Hazard. Mater. 146, 496–501.

Fuh, C.B., Lai, M., Tsai, H.Y., Chang, C.M., 2005. Impurity analysis of 1,4-dioxane in nonionic surfactants and cosmetics using headspace solid-phase microextraction coupled with gas chromatography and gas chromatography–mass spectrometry. J. Chromatogr. A 1071, 141–145.

Gaya, U.I., Abdullah, A.H., 2008. Heterogeneous photocatalytic degradation of organic contaminants over titanium dioxide: a review of fundamentals, progress and problems. J. Photochem. Photobiol. C: Photochem. Rev. 9, 1–12.

Glaze, W.H., Peyton, G.R., Lin, S., Huang, R.Y., Burleson, J.L., 1982. Destruction of pollutants in water with ozone in combination with ultraviolet radiation. II. Natural trihalomethane precursors. Environ. Sci. Technol. 16, 454–458.

Glaze, W.H., Schep, R., Chauncey, W., Ruth, E.C., Zarnoch, J.J., Aieta, E.M., Tate, C.H., McGuire, M.J., 1990. Evaluation oxidants for the removal of model taste and odour compounds from a municipal water supply. J. Am. Waterworks Assoc. 85, 79–84.

Guo, W., Brodowsky, H., 2000. Determination of the trace 1,4-dioxane. Microchem. J. 64, 173–179.

Hebert, A., Forestier, D., Lenes, D., Benanou, D., Jacob, S., Arfi, C., Lambolez, L., Levi, Y., 2010. Innovative method for prioritizing emerging disinfection by-products (DBPs) in drinking water on the basis of their potential impact on public health. Water Res. 44, 3147–3165.

Hill, R.R., Jeffs, G.E., Roberts, D.R., 1997. Photocatalytic degradation of 1 4-dioxane in aqueous solution. J. Photochem. Photobiol. A: Chem. 108, 55–58.

Imoberdorf, G., Mohseni, M., 2012. Kinetic study and modeling of the vacuum-UV photoinduced degradation of 2,4-D. Chem. Eng. J. 187, 114–122.

Isaacson, C., Mohr, T.K.G., Field, J.A., 2006. Quantitative determination of 1,4-dioxane and tetrahydrofuran in groundwater by solid phase extraction GC/MS/MS†. Environ. Sci. Technol. 40, 7305–7311.

Ishikawa, T., Yamaoka, H., Harada, Y., Fujii, T., Nagasawa, T., 2002. A general process for in situ formation of functional surface layers on ceramics. Nature 416, 64–67.

Joyner, R.A., 1912. Die Affinitätskonstante des Hydroperoxyds. Zeitschrift für anorganische Chemie 77, 103–115.

JWWA, 2011. Standard Methods for the Examination of Water. Jpn. Water Works Assoc.

Klečka, G.M., Gonsior, S.J., 1986. Removal of 1,4-dioxane from wastewater. J. Hazard. Mater. 13, 161–168.

Kransner, S.W., McGuire, M.J., Jacangelo, J.G., Patania, N.L., Reagan, K.M., Aieta, E.M., 1989. The occurrence of disinfection by-products in US drinking water. J. Am. Water Works Assoc. 81, 41–53.

Kruithof, J.C., Kamp, P.C., Martijn, B.J., 2007. UV/H_2O_2 treatment: a practical solution for organic contaminant control and primary disinfection. Ozone: Sci. Eng. 29, 273–280.

Kutschera, K., Börnick, H., Worch, E., 2009. Photoinitiated oxidation of geosmin and 2-methylisoborneol by irradiation with 254 nm and 185 nm UV light. Water Res. 43, 2224–2232.

LaVerne, J.A., 1989. The production of oh radicals in the radiolysis of water with 4He ions. Radiat. Res. 118, 201–210.

Lawton, L.A., Robertson, P.K.J., Robertson, R.F., Bruce, F.G., 2003. The destruction of 2-methylisoborneol and geosmin using titanium dioxide photocatalysis. Appl. Catal. B: Environ. 44, 9–13.

Lesage, S., Jackson, R.E., Priddle, M.W., Riemann, P.G., 1990. Occurrence and fate of organic solvent residues in anoxic groundwater at the Gloucester landfill. Can. Environ. Sci. Technol. 24, 559–566.

Lewis, B., Chestner, S., 1981. Formaldehyde in dentistry: a review of mutagenic and carcinogenic potential. J. Am. Dental Assoc. 103, 429–434.

Liao, C.-H., Gurol, M.D., 1995. Chemical oxidation by photolytic secomposition of hydrogen peroxide. Environ. Sci. Technol. 29, 3007–3014.

Lopez, A., Bozzi, A., Mascolo, G., Kiwi, J., 2003. Kinetic investigation on UV and UV/H2O2 degradations of pharmaceutical intermediates in aqueous solution. J. Photochem. Photobiol. A: Chem. 156, 121–126.

Müller, J.-P., Jekel, M., 2001. Comparison of advanced oxidation processes in flow-through pilot plants (Part I). Water Sci. Technol. 44, 303–309.

Malliarou, E., Collins, C., Graham, N., Nieuwenhuijsen, M.J., 2005. Haloacetic acids in drinking water in the United Kingdom. Water Res. 39, 2722–2730.

Marnett, L.J., Hurd, H.K., Hollstein, M.C., Levin, D.E., Esterbauer, H., Ames, B.N., 1985. Naturally occurring carbonyl compounds are mutagens Salmonella tester strain TA104. Mutat. Res./Fund. Mol. Mech. Mutagen. 148, 25–34.

Maurino, V., Calza, P., Minero, C., Pelizzetti, E., Vincenti, M., 1997. Light-assisted 1,4-dioxane degradation. Chemosphere 35, 2675–2688.

McGuire, M.J., Suffet, I.H., Radziul, J.V., 1978. Assessment of unit processes for the removal of trace organic compounds from drinking water. J. Am Water Works Assoc. 10, 565–572.

Mehrvar, M., Anderson, W.A., Moo-Young, M., 2000. Photocatalytic degradation of aqueous tetrahydrofuran, 1,4-dioxane, and their mixture with TiO_2. Int. J. Photoenergy 2, 67–80.

Mehrvar, M., Anderson, W.A., Moo-Young, M., 2002. Comparison of the photoactivities of two commercial titanium dioxide powders in the degradation of 1,4-dioxane. Int. J. Photoenergy 4, 141–146.

Oppenländer, T., 2007. Mercury-free sources of VUV/UV radiation: application of modern excimer lamps (excilamps) for water and air treatment. J. Environ. Eng. Sci. 6, 253–264.

Oppenländer, T., Sosnin, E., 2005. Mercury-free vacuum-(VUV) and UV excilamps: lamps of the future? IUVA News 7, 16–20.

Pinkernell, U., von Gunten, U., 2001. Bromate minimization during ozonation: mechanistic considerations. Environ. Sci. Technol. 35, 2525–2531.

Richardson, S.D., Plewa, M.J., Wagner, E.D., Schoeny, R., DeMarini, D.M., 2007. Occurrence, genotoxicity, and carcinogenicity of regulated and emerging disinfection by-products in drinking water: a review and roadmap for research. Mutat. Res./Rev. Mutat. Res. 636, 178–242.

Rosenfeldt, E.J., Melcher, B., Linden, K.G., 2005. UV and UV/H_2O_2 treatment of methylisoborneol (MIB) and geosmin in water. J. Water Supply: Res. Technol. – AQUA 54, 423–434.

Stefan, M.I., Bolton, J.R., 1998. Mechanism of the degradation of 1,4-dioxane in dilute aqueous solution using the UV/hydrogen peroxide process. Environ. Sci. Technol. 32, 1588–1595.

Suh, J.H., Mohseni, M., 2004. A study on the relationship between biodegradability enhancement and oxidation of 1,4-dioxane using ozone and hydrogen peroxide. Water Res. 38, 2596–2604.

Szabó, R.K., Megyeri, C., Illés, E., Gajda-Schrantz, K., Mazellier, P., Dombi, A., 2011. Phototransformation of ibuprofen and ketoprofen in aqueous solutions. Chemosphere 84, 1658–1663.

Tanabe, A., Kawata, K., 2008. Determination of 1,4-dioxane in household detergents and cleaners. J. AOAC Int. 91, 439–444.

Tanabe, A., Tsuchida, Y., Ibaraki, T., Kawata, K., 2006. Impact of 1,4-dioxane from domestic effluent on the agano and shinano rivers, Japan. Bull. Environ. Contam. Toxicol. 76, 44–51.

Thomson, J., Roddick, F., Drikas, M., 2002. Natural organic matter removal by enhanced photooxidation using low pressure mercury vapour lamps. Water Sci. Technol. 2 (5–6), 435–443.

Thomson, J., Roddick, F.A., Drikas, M., 2004. Vacuum ultraviolet irradiation for natural organic matter removal. J. Water Supply: Res. Technol. – AQUA 53, 193–206.

Weeks, J.L., Gordon, S., 1963. Absorption coefficients of liquid water and aqueous solutions in the far ultraviolet. Radiat. Res. 19, 559–567.

Zenker, M.J., Borden, R.C., Barlaz, M.A., 2003. Occurrence and treatment of 1,4-dioxane in aqueous environments. Environ. Eng. Sci. 20, 423–432.

Zhang, T., Lu, J., Ma, J., Qiang, Z., 2008. Comparative study of ozonation and synthetic goethite-catalyzed ozonation of individual NOM fractions isolated and fractionated from a filtered river water. Water Res. 42, 1563–1570.

Zoschke, K., Börnick, H., Worch, E., 2014. Vacuum-UV radiation at 185 nm in water treatment – a review. Water Res. 52, 131–145.

Zoschke, K., Dietrich, N., Börnick, H., Worch, E., 2012. UV-based advanced oxidation processes for the treatment of odour compounds: efficiency and by-product formation. Water Res. 46, 5365–5373.

Journal of Membrane Science 477 (2015) 115–122

Contents lists available at ScienceDirect

Journal of Membrane Science

journal homepage: www.elsevier.com/locate/memsci

Hydraulically irreversible membrane fouling during coagulation–microfiltration and its control by using high-basicity polyaluminum chloride

Masaoki Kimura [a], Yoshihiko Matsui [b,*], Shun Saito [a], Tomoya Takahashi [a], Midori Nakagawa [a], Nobutaka Shirasaki [b], Taku Matsushita [b]

[a] Graduate School of Engineering, Hokkaido University, N13W8, Sapporo 060-8628, Japan
[b] Faculty of Engineering, Hokkaido University, N13W8, Sapporo 060-8628, Japan

ARTICLE INFO

Article history:
Received 30 October 2014
Received in revised form
21 December 2014
Accepted 22 December 2014
Available online 2 January 2015

Keywords:
Ceramic
Foulant
Silicate
Coagulant
Basicity

ABSTRACT

The extent of hydraulically irreversible membrane fouling in a coagulation–filtration system depends on several factors, including properties of the coagulant. Effects of polyaluminum chloride (PACl) coagulant properties, specifically basicity and sulfation, were investigated by conducting long-term direct filtration experiments. Elemental analysis determined Al and Si to be the major foulants, though the Si/Al ratios of the foulants differed from those of coagulated floc particles. While floc particle size depended on the concentrations of sulfate ions and polymeric species in the PACls, floc-size changes did not affect transmembrane pressure (TMP) buildup and thus did not affect irreversible fouling. Differences in PACl basicity, which affected the distribution of aluminum species, resulted in changes to the degree of irreversible fouling.

Pretreatment with high-basicity (71%) PACl was superior to pretreatment with normal-basicity (51%) PACl in reducing irreversible fouling and attenuating TMP buildup during filtration. Higher basicities resulted in less Al breakthrough and a decrease in the Si/Al ratio of the foulants. However, TMP buildup was the same for PACls with basicities of 71% and 90%; therefore, TMP buildup is not simply related to Al breakthrough and deposition. Increasing the basicity of PACls would be an effective way to reduce the amount of foulant deposited on the membrane by decreasing the amount of aluminum that passes through the membrane.

1. Introduction

Coagulation, adsorption, and oxidation are widely used as pretreatment processes for microfiltration (MF) in water purification to alleviate membrane fouling and enhance the removals of micropollutants and disinfection byproduct precursors [1]. In MF with ceramic membranes, coagulation–flocculation with polyaluminum chloride (PACl) is a successful pretreatment for removing soluble substances and reducing the decrease in membrane permeability during long-time operation [2]. This process is commonly used in full-scale water treatment. Coagulation pretreatment destabilizes and agglomerates the colloidal and particulate foulants, increasing their size and thereby mitigating pore constriction and blockage and the formation of a porous cake layer. Additionally, increased particle size reduces the specific cake resistance, according to the Carman–Kozeny relationship, and thus increases permeability. However, membrane fouling is not completely avoided since aquatic colloids are not removed, which cause fouling by narrowing or blocking membrane pores, and substances retained on the membrane that form a gel or cake layer still contribute resistance.

The permeability of the cake layer formed from floc particles during coagulation has been extensively studied for dependence on floc size, strength, and fractal structure [3–5]. Coagulated flocs with a high fractal dimension have low compressibility, leading to low membrane permeability [6]. Other studies, however, found high compressibility in flocs related to a higher specific resistance of the cake layer [7,8]. Coagulated flocs with a high fractal dimension formed by PACl have a more compact structure than flocs formed by alum [9]. Therefore, the MF membrane permeability deteriorates more severely during PACl coagulation than during alum coagulation due to the higher specific resistance of the cake layer. Liu et al. [10], in contrast, report that floc particles of a high fractal dimension as well as a large size formed by two-stage coagulant dosing mitigated TMP development more than those formed by a single dose. The strength (resistance toward shear stress) of floc particles formed by coagulation also plays an important role in the permeability of the cake layer

* Corresponding author. Tel./Fax: +81 11 706 7280.
E-mail address: matsui@eng.hokudai.ac.jp (Y. Matsui).

http://dx.doi.org/10.1016/j.memsci.2014.12.033
0376-7388/

[11–13]. The increase in transmembrane pressure (TMP) in an ultrafiltration (UF) system is lower with floc breakage, which lowers the fractal dimension of flocs, than without breakage [14]. Xu and Gao [3], however, reported that an increased shear for floc breakage considerably decreased the floc size and increased the floc compactness, thus increasing resistance and lowering the permeability of the cake layer. Therefore, an increase in floc strength could enhance the permeability of the cake layer [4]. Overall, findings on the relationship of floc characteristics to membrane performance are not consistent, though it is clear the structure of the cake layer plays an important role in membrane permeability.

In a ceramic membrane MF system, the permeability of the cake layer may not be a crucial issue, because an integrated, intensive, hydraulic backwash process would eject most of the cake layer. After coagulation, the affinity of the membrane for destabilized contaminants and their aggregates is lower than without coagulation, which leads to a more effective backwash. Hence, with an integrated, hydraulic backwash, the degree of fouling from cake layer formation would be minimized. Hydraulically irreversible fouling is the main concern in full-scale membrane filtration facilities because it determines energy consumption for long-term membrane filtration and affects the sustainable operation of the facility. Irreversible fouling is caused by contaminants that do not react with or adsorb to hydrolytic species formed by the coagulant and thus are not destabilized [15]. Many studies have been conducted to better understand the behavior of membrane foulants and elucidate fouling mechanisms, but these studies have seldom identified practical solutions to the membrane-fouling problem.

A limited amount of research has concerned the extent to which different coagulant types might be exploited to most effectively reduce the extent of irreversible fouling. Tran et al. [16] reported that polysilicato-iron coagulants were better at mitigating irreversible fouling than aluminum-based coagulants at a higher dose while aluminum-based coagulants worked better at a lower dose. Their study suggests that the effect on membrane fouling is a complex phenomenon where many factors including the residual DOC and the property of small-size flocs influence the fouling to various extents. Membrane fouling may also be caused by hydrolytic species of coagulants, though it has not been fully studied [1]. The key consideration is that coagulant characteristics required for membrane pretreatment are not necessarily the same as those for coagulation and settling. Conventional coagulation is designed to form large-size floc particles that settle out, whereas, for membrane pretreatment, coagulation should allow for direct filtration of floc that results in improved filtrate water quality and alleviates membrane fouling.

In this study, we investigated five PACl coagulants suitable for direct MF. The effect of PACl properties (basicity and sulfated/non-sulfated) on hydraulically irreversible membrane fouling (hereafter called irreversible fouling), which results in a long-term TMP rise, was studied, in particular, by focusing on the residual aluminum concentration in filtrates and aluminum deposits on membranes.

2. Materials and methods

2.1. Coagulants

Four PACls were obtained from the Taki Chemical Co. (Kakogawa, Japan): conventional normal-basicity (51%) sulfated PACl (designated as PACl-51s), high-basicity (71%) sulfated PACl (PACl-71s), high-basicity (71%) nonsulfated PACl (PACl-71), and very-high-basicity (90%) nonsulfated PACl (PACl-90). A second very-high-basicity (90%) nonsulfated PACl (PACl-90b) was prepared in the authors' laboratory by the base titration method using NaOH (0.3 M) and $AlCl_3$ (0.5 M) [17]. The distributions of aluminum species in the coagulants were determined by the ferron method [17]. These species were assumed to be monomeric, polymeric, and colloidal aluminum species on the basis of their reaction rates with ferron reagent (8-hydroxy-7-iodo-5-quinolinesulfonic acid; Wako Pure Chemical Industries, Osaka, Japan), denoted Ala, Alb, and Alc, respectively [18]. Ala denotes aluminum species that reacted with ferron instantaneously (within 30 s); Alb denotes species that reacted with ferron within 120 min; and Alc denotes species that did not react. Properties of the PACls are listed in Table 1S (Supplementary data).

2.2. Pilot-scale MF system

Experiments were conducted with the coagulation-direct MF pilot plant at the Water Quality Center of the Sapporo Waterworks Bureau, Japan. The plant has two parallel lines (Lines A and B) with the same

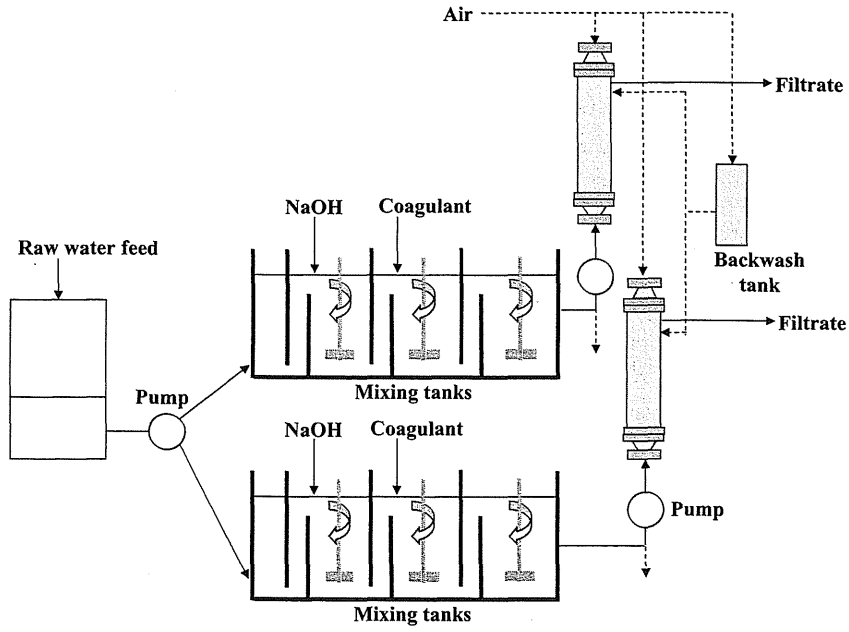

Fig. 1. Pilot-scale MF systems.

configuration, each consisting of coagulation mixing tanks, a feed pump, a membrane module, and a hydraulic backwash unit in series (Fig. 1). The two lines were operated in parallel under identical conditions except for coagulant type and dosage of caustic soda for pH control, which enabled direct comparison of the experiments. The coagulation process was performed in rapidly and slowly stirred mixing tanks with detention times of 7.3 and 12.5 min, respectively. Mixing intensities were 60 rpm (G=68.5 s^{-1}) and 20 rpm (G=13.3 s^{-1}) unless otherwise noted. Each line has a small membrane module containing a tubular, ceramic monolith membrane element (nominal pore size, 0.1 μm; 55 channels; diameter, 3 cm; length, 10 cm; effective filtration area, 0.043 m^2; Metawater Co., Tokyo, Japan). The element was specially designed for small-scale experiments; in comparison, the membrane element used for the full-scale filtration plant has a membrane surface area of 25 m^2, a diameter of 1800 mm, and a length of 1.5 m. Before each filtration run, the membrane element was chemically-cleaned and, after housing the module, the initial permeability was checked. The module was configured for dead-end filtration with constant flow to the membrane module (filtration rate, 0.125 m/h) by positive pressure. The membranes were hydraulically backwashed every hour from the filtrate side with membrane permeate at a pressure of 500 kPa for 20 s, and the retentate was ejected by pressurized water and air. Feed pressure, raw water turbidity, water temperature, and coagulation pH were monitored continuously, and the data were stored. Coagulant dose was automatically adjusted as a function of raw water turbidity [dosage/(mg-Al/L)= 1.06 for 0–7 NTU, dosage/(mg-Al/L)=0.151 × turbidity/NTU for 7–14 NTU, dosage/(mg-Al/L)=0.034 × turbidity/NTU+1.65 for 14–140 NTU; these formulas were determined from the PACl dosage–turbidity relationship obtained at the Moiwa Water Treatment Plant, which treats the same raw water]. Coagulation pH was controlled at a constant value by the automatic dosage of caustic soda, except for the first set of runs (Run 1). Plant operation was continued either for 25–35 days or until the TMP reached about 100 kPa. In some cases, operation was terminated due to cessation of raw water flow from the Water Quality Center. During plant operation, samples of coagulated waters before direct MF were taken manually and immediately filtered through organic membranes (polycarbonate, Isopore, Millipore Corp.) of the same nominal pore size, 0.1 μm, as that of the ceramic membrane. For some runs, samples were filtered through organic membranes of various molecular mass cutoffs (500 Da, cellulose acetate, Amicon-Y, Millipore Corp; 1, 3, 10, and 100 kDa, regenerated cellulose, Ultracell-PL, Millipore Corp.). In total, 11 runs of parallel filtrations were conducted (Table 2S, Supplementary data). Additionally, for supplementary membrane filtrate sampling and foulant analysis, seven pairs of runs were carried out with PACl-60s (sulfated, basicity 60%, Taki Chemical Co.), PACl-65s (sulfated, basicity 65%, Taki Chemical Co.) and PACl-85 (nonsulfated, basicity 85%, Taki Chemical Co.).

2.3. Water quality

The plant treated Toyohira River water that was taken at Moiwa Dam (42.966182N, 141.269428E) and transported to the Water Quality Center through pipelines. The concentrations of dissolved organic carbon (DOC) and aluminum in the water were determined by the UV/persulfate oxidation method (Sievers 900 TOC Analyzer, GE Analytical Instruments, Boulder, CO, USA) and inductively coupled plasma mass spectrometry (ICP-MS, HP-7700, Agilent Technologies, Inc., Santa Clara, CA, USA), respectively. The characteristics of the raw water and the coagulation pH are listed in Table 2S (supplementary data).

2.4. Chemical cleaning of membrane and foulant analysis

After the final hydraulic backwashing in a filtration run, the membrane element was removed from the module and chemically cleaned by repeating the following soak cycle three times: sulfuric acid (0.02 N) for 18 h, Milli-Q water (Millipore Corp.) for 1 min, sodium hypochlorite (1500 mg-Cl_2/L) for 18 h, and Milli-Q water for 1 min. The spent cleaning solutions and Milli-Q waters were analyzed for organic C (Shimadzu TOC-5000A, Kyoto, Japan), Al, Si, Fe, Mn, and Ca (ICP-MS, HP-7700, Agilent Technologies, Inc.) to determine the concentrations of membrane foulants. Al and Si elemental analyses were conducted on the floc particles retained on the organic membrane filter from the manually collected and filtered samples (PTFE, 0.1 μm, Omnipore, Millipore Corp.) and on the ceramic membrane retentates ejected in the hydraulic backwash process.

3. Results and discussion

3.1. Effect of high-basicity (71%) PACl

Five pairs of runs (parallel filtrations) were conducted with PACl-71s in one line and PACl-51s in the other line. The rates of TMP buildup over the period of operation were lower when feedwater was pretreated with PACl-71s than with PACl-51s (Fig. 2). Even at pH 7.5, which sees more membrane fouling, PACl-71s lowered the rate of TMP buildup (Fig. 2C). Additional runs in which coagulation was conducted at pH 7.0 and pH 7.1 showed similar results, with the TMP following PACl-71s coagulation remaining at a low level throughout the period of operation (Fig. 1S, Supplementary data). The consistent results in the five pairs of runs indicate that the difference in the TMP buildups between PACl-71s and PACl-51s was not due to any very slight difference in initial membrane permeability. Moreover, PACl-71s was used in Line B in Runs 1, 2, and 3 and in Line A in Runs 4 and 5. Therefore, the difference in TMP rise is not due to any inherent characteristics of the line, including the membrane element used. We interpret the low rate of TMP buildup in the filtration with periodic backwash as mild irreversible fouling. The high rate of TMP buildup is characterized as severe irreversible fouling. Floc particle size is a key characteristic that affects reversible fouling, but may not be related to irreversible fouling. Fine floc particles were more often observed in the mixing tank after the addition of PACl-71s than after the addition of PACl-51s (Fig. 2S, Supplementary data), but addition of PACl-71s yielded a lower rate of TMP rise. The effects of floc particle size are further explored in Section 3.3.

The masses of Al and other elements extracted from the fouled membrane by chemical cleaning are shown in Fig. 3. The amounts of Al and Si were the largest among the elements extracted, followed by organic C and Ca, suggesting that the irreversible foulants were mainly composed of these elements. The low relative loadings of organic C indicate natural organic matter (NOM) was not a main cause of membrane fouling: this might be due to the low DOC concentrations in the raw waters (Table 2S). Loadings of Al and Si on the membrane were lower with PACl-71s pretreatment than with PACl-51s pretreatment (Fig. 3S, Supplementary data). Therefore, the lower TMP rise observed with PACl-71s pretreatment could possibly be due to lower loading rates of compounds composed of these elements.

The residual aluminum in the filtrate was lower with PACl-71s pretreatment than with PACl-51s pretreatment (Runs 2–5 of Fig. 4: the comparison in Run 1 was not appropriate because pH was not stable during the experiment and pH of PACl-71s coagulation was often higher than pH of PACl-51s coagulation). This was due to less monomeric aluminum (Ala) in PACl-71s [17]; the percentages of Ala in PACl-71s and PACl-51s are 18.3% and 43.5%, respectively (Table 1S, Supplementary data). Similar residual aluminum results were also seen in the filtrates of the manually collected samples through a polycarbonate membrane, which did not exhibit adsorption ability, with fixed straight pores of the size 0.1 μm, the same as that of the ceramic membrane [19] (Fig. 4S, Supplementary data). Therefore, it can be interpreted that the concentration of

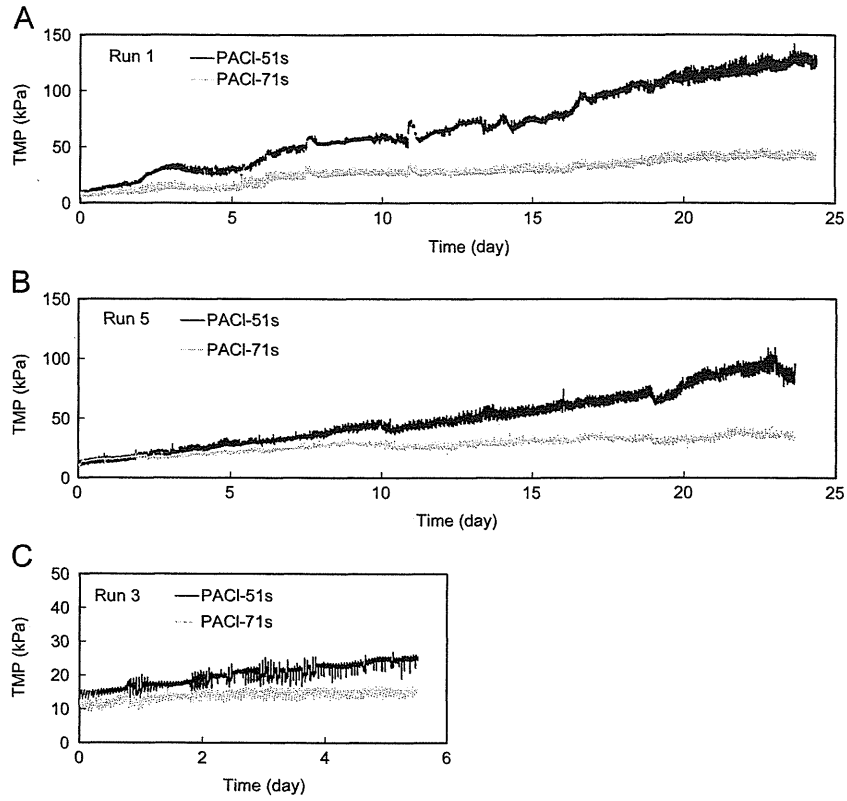

Fig. 2. Comparison of TMP variations during microfiltration after PACl-51s and PACl-71s coagulations: (A) Run 1 (coagulation pH 6.1–7.3); (B) Run 5 (coagulation pH 7.0); (C) Run 3 (coagulation pH 7.5).

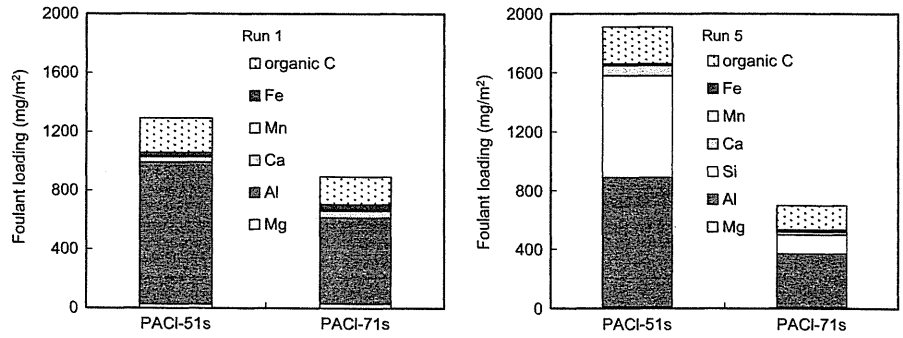

Fig. 3. Elemental compositions of membrane foulants recovered in chemical cleaning agents (Si was not analyzed for Run 1).

small-size aluminum passing through the ceramic membrane was lower with PACl-71s pretreatment than with PACl-51s pretreatment. Some of the small-size aluminum species passing through the membrane pores might be retained by chance in membrane pores and then foul the membrane. We then thought that the low extent of membrane fouling with PACl-71s pretreatment might have been related to a low aluminum concentration. Molecular weight fractionation with organic MF and UF membranes revealed that the difference in aluminum concentration in the filtrates with the PACl-71s and PACl-51s pretreatments was in the size range >500 Da (Fig. 5S, Supplementary data). This result is in accordance with previous jar test results that showed that PACl-71s lowered residual aluminum in the size range >500 Da [17]. The DOC in the filtrate was also lower with PACl-71s pretreatment than with PACl-51s pretreatment (Fig. 6S), and the loadings of organic carbon on the membrane were lower with PACl-71s pretreatment than with PACl-51s pretreatment (Fig. 3S). Therefore,

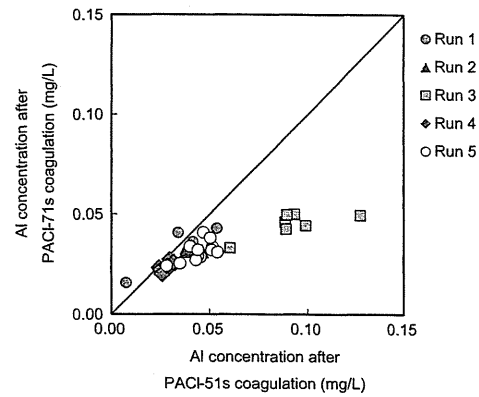

Fig. 4. Aluminum concentrations in the MF filtrates after PACl-71s and PACl-51s coagulations.

the high NOM removal capability of PACl-71s might also be related to the low rate of TMP buildup.

3.2. Effect of very-high-basicity (90%) PACl

We tested two very-high-basicity (90%) PACls (PACl-90b and PACl-90). PACl-90b had a higher content of Alb, which has a high charge neutralization capacity [20,21], than PACl-90 or PACl-71s. Kimura et al. [17] reported that very-high-basicity (90%) PACls can decrease the residual Al concentration much more than 71% basicity PACls because 90%-basicity PACls only contain a very small amount of monomeric aluminum species (Ala). Given the lower TMP rise of PACl-71s with respect to PACl-51s, it was suspected that the extent of membrane fouling was related to residual Al concentration in the filtrate, with lower residual leading to lower fouling and less TMP buildup. The percentages of Ala in PACl-90, PACl-90b, PACl-71s, and PACl-51s are 0.4%, 1.2%, 18.3%, and 43.5%, respectively (Table 1S). Therefore, membrane fouling should be less with PACl-90b and PACl-90 than with PACl-71s. Three pairs of runs were carried out. Results for two pairs of the runs are shown in Fig. 5, and results for the third pair, which had a shorter operational time, are shown in Fig. 7S (Supplementary data). In all runs, coagulations with PACl-90b and PACl-90 yielded a similar TMP buildup over the entire operation time as coagulation with PACl-71s. Nonsulfated PACls of basicities 71% and 90% (PACl-71 and PACl-90) also saw no difference in TMP buildup (Fig. 8S, Supplementary data). Loadings of Al on the membrane were not different between PACls with basicities of 90% (PACl-90 and PACl-90b) and 71% (PACl-71s) (Fig. 9S, Supplementary data).

While further reduction of the residual aluminum concentration (< 0.009 mg/L) was successfully achieved – as expected, aluminum concentrations in the filtrates dramatically decreased as basicity increased from 71% to 90% (Fig. 6) – it was not accompanied by a further attenuation of TMP buildup. Thus, increasing basicity to 90% and changing the aluminum species distribution did not further improve permeability. This result suggests that the quantity of small-size aluminum species passing through the membrane pores was not the main cause of the membrane's fouling. Instead, the aluminum species that did not pass through the membrane pores might have caused external membrane fouling by forming a gel layer, which probably consisted mostly of aluminum, on top of the separation layer of the membrane. This differs from pretreatment with a PACl with a basicity of 51%, where external membrane fouling may have been caused by formation of a gel layer and internal membrane fouling could have been caused by internal deposition of aluminum associated with particles smaller than the membrane pore size. Therefore, the characteristics of the membrane foulant might depend on the basicity of the PACl used for coagulation pretreatment. The DOC in the filtrate was slightly higher with 90%-basicity PACl pretreatment than with 71% pretreatment (Fig. 10S). The loading of organic carbon was also slightly higher with 90%-basicity PACl pretreatment. Therefore, the effect of the low aluminum concentration with 90%-basicity PACls might possibly be canceled out with its high DOC, which eventually resulted in the similar TMP buildup rate of PACl-90 to PACl-71s. Experiments using raw water of high NOM concentration are granted to more clearly elucidate the effect of PACl characteristics on the NOM removal and fouling [22].

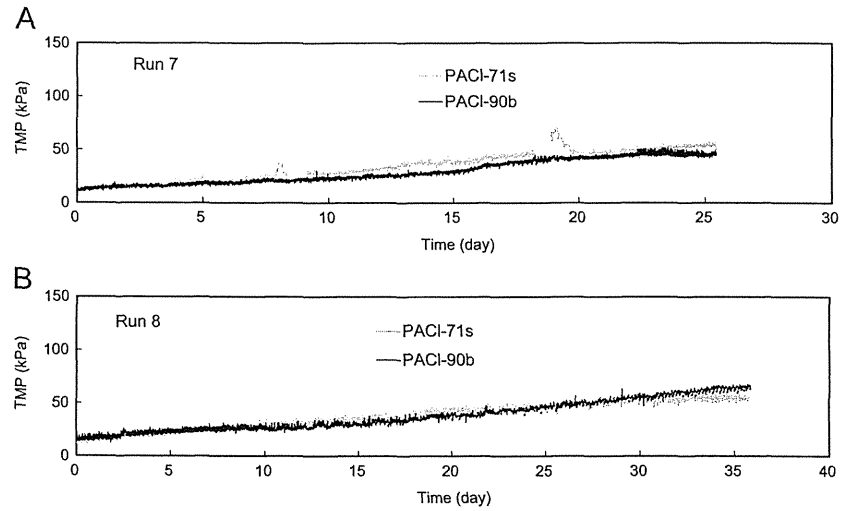

Fig. 5. Comparison of TMP variations during microfiltration after PACl-90b and PACl-71s coagulations: (A) Run 7 (coagulation pH 7.5); (B) Run 8 (coagulation pH 7.5).

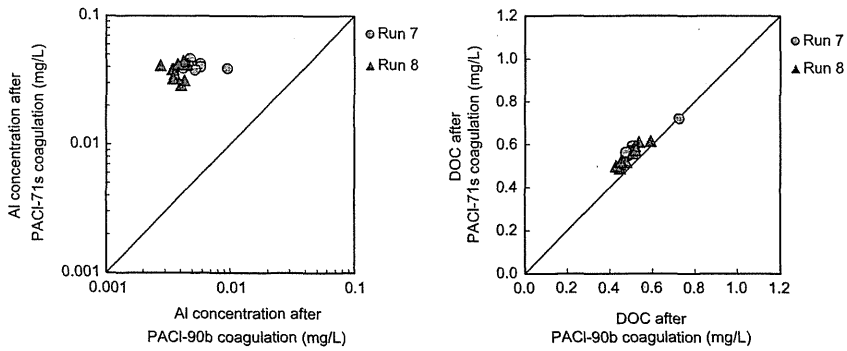

Fig. 6. Aluminum and DOC concentrations in the MF filtrates after PACl-90b and PACl-71s coagulations.

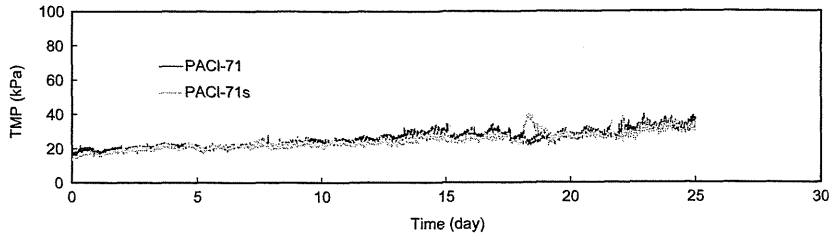

Fig. 7. Comparison of TMP variations during microfiltration after PACl-71 and PACl-71s coagulations. Run 11 (coagulation pH 7.5).

3.3. *Effect of sulfate ion in PACl*

Sulfate is often added to PACls because it suppresses charge reversal and enhances flocculation performance [25]. Pretreatment with PACl-90b produced very fine floc particles, whereas pretreatment with PACl-71s produced larger floc particles (Fig. 11S, Supplementary data). The very fine floc particles formed by PACl-90b are probably due to the absence of sulfate ion in the PACl. Therefore, it seemed likely that pretreatment with very-high-basicity (90%) PACls would cancel out the positive effect from the lower residual Al concentration with a possible negative effect from the very fine floc particles.

To further study the effect of floc size on filtration, we compared PACl-71s and PACl-71 – two PACls with the same basicity and aluminum species distribution but with or without the sulfate ion in their structures (Table 1S). PACl-71 formed more very fine floc particles than did PACl-71s (Fig. 12S, Supplementary data), however, the TMP variations during filtration were similar (Fig. 7). This result indicates that the very fine floc particles formed by the nonsulfated PACls (PACl-90b and PACl-71) did not have a negative impact on the irreversible fouling, leaving only the positive effect of TMP mitigation. This is further supported by microphotographs that show particles larger than a few microns, much larger than the membrane pore size (0.1 μm), and therefore would not plug the membrane pores. Lastly, the chemical constitution of the irreversible foulant was different from that of the floc particles (see Section 3.4) thus floc particles were not directly related to the irreversible fouling. Here we would like to note that our results of the little floc-size effect were obtained on the experiments of dead-end mode filtration. For other hydro-dynamic conditions, such as cross-flow mode, the further study is needed.

So far, the results can be generalized as follows: for a MF system that includes an intensive hydraulic backwash process, coagulants that produce floc particles much larger than the membrane pore size are more than enough for pretreatment. Such a coagulant property is actually required for pretreatment before sedimentation or for enhancing cake layer permeability in membrane systems without a hydraulic backwash. We therefore infer that a high-basicity nonsulfated PACl functions successfully as such a coagulant provided that it retains the capacity to neutralize charge.

Furthermore, inclusion of sulfate ions in PACls with high aluminum content influences the PACls' long-term chemical stability, so the sulfate ion concentration in practically applied PACls with Al content $>5\%$ (w/w) is typically limited to a few percent to allow the storage periods >6 months. Therefore, the success of the high-basicity nonsulfated PACl gives merit to its practical application in terms of a long storage period.

3.4. *Aluminum and silicate loads on membrane*

The spent membrane-cleaning solutions from filtration runs, including short runs terminated forcibly by cessation of raw water supply, were analyzed for the major irreversible membrane foulants, Al and Si. The ratios of Si/Al were plotted against the basicity of the PACls used for the coagulation pretreatment (Fig. 8). The Si/Al ratios decreased with increasing basicity, suggesting that the characteristics of the membrane foulant differ depending on the basicity of PACl used for the coagulation pretreatment. Therefore, we infer that increasing the PACl basicity not only decreases the concentration of aluminum passing through the membrane and thereby possibly reducing the load of the major foulant, aluminum, but also it changes the characteristics of membrane foulant and through this, may contribute to the attenuation of the TMP buildup.

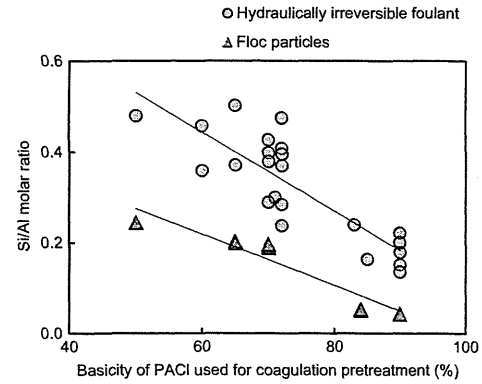

Fig. 8. Comparison of Si/Al molar ratios (Runs 6–9, 11, 12 and 17–19. Coagulation pH was 7.5–7.8).

The feed water to the membrane contained aluminum and silicate at very different concentrations. The aluminum concentration (around 1.2 mg/L on average) was much lower than the Si concentration (around 6.6 mg/L), and the Si/Al molar ratio was about 5.3 for the feed water. The Si/Al ratios of the irreversible membrane foulant varied from 0.5 to 0.2, depending on the basicity of the PACls. Since most of the aluminum in the feed water to the membrane was in a suspended form (floc), whereas the silicate was in a soluble form, a small portion of the silicate might have been incorporated into the aluminum that precipitated after the PACl was dosed. However, the extent of incorporation is low for high-basicity PACl because the aluminum was pre-neutralized in the PACl solution. The Si/Al ratio of the irreversible membrane foulant at each basicity was also higher than that of the floc particles that were ejected by the hydraulic backwash, the highest ratio of which was 0.2. The difference of the Si/Al ratio suggests that the irreversible foulant did not originate from floc particles, even though the irreversible foulant also consisted mostly of aluminum. Adding to the fact that floc size did not affect the extent of irreversible fouling, this further shows that floc particles are not directly related to irreversible fouling.

The higher Si/Al ratios of the irreversible foulant for the lower-basicity PACls suggest that Si plays a role in membrane fouling. A stability diagram (Geochemist's Workbench, ver. 6, RockWare, Inc., Golden, CO, USA) for the chemistry of the membrane feedwater suggests that kaolinite [$Al_2Si_2O_5(OH)_4$] was the final stable species; the aqueous solubility of kaolinite is much lower than that of gibbsite [$Al(OH)_3$] [23]. The Si/Al molar ratio of kaolinite is 1.0, a value closer to

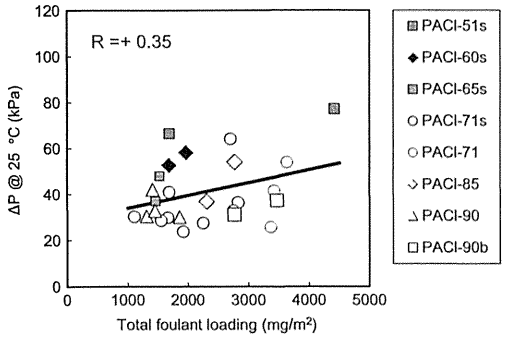

Fig. 9. Relationship between TMP normalized at 25 °C and foulant loading (Runs 5–9, 11, 12 and 17–19). The total foulant loading was calculated with the assumption that Al and Si mainly exist in the forms of $Al_2Si_2O_5(OH)_4$ according to Section 3.1, the excess Al in the form of $Al(OH)_3$ if Al/Si > 1, the excess Si in the form of SiO_2 if Si/Al > 1, Ca in the form of $Ca(OH)_2$, Mg in the form of $Mg(OH)_2$, Fe in the form of $Fe(OH)_3$, and Mn in the form of $MnO(OH)_2$; the carbon content of organic matter was 51%.

that of the irreversible foulant than to that of the floc particles. We infer that aluminum silicate hydroxide, which is chemically similar to kaolinite but amorphous, probably accumulated on top of and inside the membrane, thereby irreversibly fouling the membrane.

Quantification of total foulant loads sheds light on its relationship to TMP rise; however, it requires information about the chemical structures of the foulants and such information is scant. The total loads shown in Fig. 9 were calculated on the assumption that the Si existed mainly in compounds characterized by the stoichiometry of $Al_2Si_2O_5(OH)_4$, the surplus of Al over Si was in the form of $Al(OH)_3$, Ca was in the form of $Ca(OH)_2$, Mg was in the form of $Mg(OH)_2$, Fe was in the form of $Fe(OH)_3$, and Mn was in the form of $MnO(OH)_2$. Carbon was assumed to account for 50% of the organic matter [24]. The positive correlation between the total foulant loading and TMP suggests that the quantity of total foulant loading is an index for TMP. However, the correlation was not high ($r = +0.35$, Fig. 9). When compared at the same loading, the TMPs of direct MF after coagulation with normal basicities (50% and 60%) were higher than the TMPs associated with high and very-high basicities (> 70%). This correlation suggests the rise in TMP may to some extent be related to the quantity of total foulant loading on the membrane, but altogether, the characteristics of membrane foulants depend primarily on the PACls used for coagulation pretreatment.

4. Summary

1) In ceramic MF with PACl coagulation pretreatment, long-term development of TMP caused by hydraulically irreversible fouling followed the order PACl-90b = PACl-90 = PACl-71s < PACl-51s. Use of high-basicity (71%) PACl coagulant (PACl-71s) reduced hydraulically irreversible fouling and attenuated long-term development of TMP compared with normal-basicity (51%) PACl coagulants (PACl-51s). The use of very-high-basicity (90%) PACls (PACl-90b and PACl-90), however, did not result in a reduction of long-term TMP buildup beyond that obtained with PACl-71s.
2) Aluminum concentrations in the filtrates were in the following order: PACl-90 = PACl-90b < PACl-71s < PACl-51s. This order paralleled the order of Ala content in the PACls. The lower aluminum passage following pretreatment with a high-basicity PACl correlated with less membrane fouling. PACl-90 and PACl-71s exhibited similar long-term TMP buildup, suggesting that the characteristics of the membrane foulant differed from the normal basicity PACl of 51%. This conclusion was also supported by the fact that the Si/Al ratio of hydraulically irreversible foulants, which consisted mostly of Al and Si, decreased with increasing basicity of the PACl used for coagulation pretreatment.
3) The hydraulically irreversible foulants differed in terms of Si/Al ratios compared to floc particles. Additionally, while floc size was a function of the concentration of sulfate ions and polymeric species in the PACls, it did not affect the reduction of hydraulically irreversible fouling. Therefore, the floc particles were not directly related to hydraulically irreversible fouling.

Acknowledgments

This study was supported by a Grant-in-Aid for Scientific Research S (24226012) from the Japan Society for the Promotion of Science.

Appendix A. Supporting information

Supplementary data associated with this article can be found in the online version at http://dx.doi.org/10.1016/j.memsci.2014.12.033.

References

[1] H. Huang, K. Schwab, J.G. Jacangelo, Pretreatment for low pressure membranes in water treatment: a review, Environ. Sci. Technol. 43 (2009) 3011–3019.
[2] Y. Matsui, T. Matsushita, T. Inoue, M. Yamamoto, Y. Hayashi, H. Yonekawa, Y. Tsutsumi, Virus removal by ceramic membrane microfiltration with coagulation pretreatment, Water Sci. Technol. 3 (2003) 93–99.
[3] W. Xu, B. Gao, Effect of shear conditions on floc properties and membrane fouling in coagulation/ultrafiltration hybrid process—the significance of Alb species, J. Membr. Sci. 415–416 (2012) 153–160.
[4] W. Xu, B. Gao, Y. Wang, Q. Zhang, Q. Yue, Influences of polysilicic acid in Al13 species on floc properties and membrane fouling in coagulation/ultrafiltration hybrid process, Chem. Eng. J. 181–182 (2012) 407–415.
[5] Y. Matsui, H. Hasegawa, K. Ohno, T. Matsushita, S. Mima, Y. Kawase, T. Aizawa, Effects of super-powdered activated carbon pretreatment on coagulation and trans-membrane pressure buildup during microfiltration, Water Res. 43 (2009) 5160–5170.
[6] M.H. Cho, C.H. Lee, S. Lee, Influence of floc structure on membrane permeability in the coagulation–MF process, Water Sci. Technol. 51 (2005) 143–150.
[7] Y.H. Choi, H.S. Kim, J.H. Kweon, Role of hydrophobic natural organic matter flocs on the fouling in coagulation–membrane processes, Sep. Purif. Technol. 62 (2008) 529–534.
[8] B. Zhao, D. Wang, T. Li, C. Huang, Effect of floc structure and strength on membrane permeability in the hybrid coagulation-microfiltration process, Water Sci. Technol. 11 (2011) 97–105.
[9] J. Wang, J. Guan, S.R. Santiwong, T.D. Waite, Characterization of floc size and structure under different monomer and polymer coagulants on microfiltration membrane fouling, J. Membr. Sci. 321 (2008) 132–138.
[10] T. Liu, Z.-l. Chen, W.-Z. Yu, J.-m. Shen, J. Gregory, Effect of two-stage coagulant addition on coagulation–ultrafiltration process for treatment of humic-rich water, Water Res. 45 (2011) 4260–4268.
[11] T.D. Waite, A.I. Schäfer, A.G. Fane, A. Heuer, Colloidal fouling of ultrafiltration membranes: impact of aggregate structure and size, J. Colloid Interface Sci. 212 (1999) 264–274.
[12] E. Barbot, S. Moustier, J. Bottero, P. Moulin, Coagulation and ultrafiltration: understanding of the key parameters of the hybrid process, J. Membr. Sci. 325 (2008) 520–527.
[13] B. Zhao, D. Wang, T. Li, C.W.K. Chow, C. Huang, Influence of floc structure on coagulation–microfiltration performance: effect of Al speciation characteristics of PACls, Sep. Purif. Technol. 72 (2010) 22–27.
[14] W. Yu, T. Liu, J. Gregory, L. Campos, G. Li, J. Qu, Influence of flocs breakage process on submerged ultrafiltration membrane fouling, J. Membr. Sci. 385–386 (2011) 194–199.
[15] Y. Chen, B.Z. Dong, N.Y. Gao, J.C. Fan, Effect of coagulation pretreatment on fouling of an ultrafiltration membrane, Desalination 204 (2007) 181–188.
[16] T. Tran, S. Gray, R. Naughton, B. Bolto, Polysilicato-iron for improved NOM removal and membrane performance, J. Membr. Sci. 280 (2006) 560–571.
[17] M. Kimura, Y. Matsui, K. Kondo, T.B. Ishikawa, T. Matsushita, N. Shirasaki, Minimizing residual aluminum concentration in treated water by tailoring properties of polyaluminum coagulants, Water Res. 47 (2013) 2075–2084.
[18] D. Wang, W. Sun, Y. Xu, H. Tang, J. Gregory, Speciation stability of inorganic polymer flocculant–PACl, Colloids Surf. A 243 (2004) 1–10.
[19] Y. Matsui, T.B. Ishikawa, M. Kimura, K. Machida, N. Shirasaki, T. Matsushita, Aluminum concentrations of sand filter and polymeric membrane filtrates: a comparative study, Sep. Purif. Technol. 119 (2013) 58–65.

[20] B.-Y. Gao, Y.-B. Chu, Q.-Y. Yue, B.-J. Wang, S.-G. Wang, Characterization and coagulation of a polyaluminum chloride (PAC) coagulant with high Al13 content, J. Environ. Manag. 76 (2005) 143–147.
[21] N. Parthasarathy, J. Buffle, Study of polymeric aluminium(III) hydroxide solutions for application in waste water treatment. Properties of the polymer and optimal conditions of preparation, Water Res. 19 (1985) 25–36.
[22] H. Zhao, H. Liu, C. Hu, J. Qu, Effect of aluminum speciation and structure characterization on preferential removal of disinfection byproduct precursors by aluminum hydroxide coagulation, Environ. Sci. Technol. 43 (2009) 5067–5072.
[23] K. Ohno, Y. Matsui, M. Itoh, Y. Oguchi, T. Kondo, Y. Konno, T. Matsushita, Y. Magara, NF membrane fouling by aluminum and iron coagulant residuals after coagulation–MF pretreatment, Desalination 254 (2010) 17–22.
[24] International Humic Substance Society, Elemental Compositions and Stable Isotopic Ratios of IHSS Samples, 2013.
[25] A. Amirtharaja, C.R. O'Melia, Coagulation processes: destabilization, mixing, and flocculation, in: F.W. Pontius (Ed.), Water Quality & Treatment, 4th ed., McGraw-Hill, 1990.

WATER RESEARCH 68 (2015) 227–237

Available online at www.sciencedirect.com

ScienceDirect

journal homepage: www.elsevier.com/locate/watres

Removal of iodide from water by chlorination and subsequent adsorption on powdered activated carbon

Mariya Ikari [a], *Yoshihiko Matsui* [b,*], *Yuta Suzuki* [a], *Taku Matsushita* [b], *Nobutaka Shirasaki* [b]

[a] *Graduate School of Engineering, Hokkaido University, N13W8, Sapporo 060-8628, Japan*
[b] *Faculty of Engineering, Hokkaido University, N13W8, Sapporo 060-8628, Japan*

ARTICLE INFO

Article history:
Received 5 June 2014
Received in revised form
7 October 2014
Accepted 8 October 2014
Available online 16 October 2014

Keywords:
Iodide
Iodate
SPAC
PAC
NOM

ABSTRACT

Chlorine oxidation followed by treatment with activated carbon was studied as a possible method for removing radioactive iodine from water. Chlorination time, chlorine dose, the presence of natural organic matter (NOM), the presence of bromide ion (Br^-), and carbon particle size strongly affected iodine removal. Treatment with superfine powdered activated carbon (SPAC) after 10-min oxidation with chlorine (1 mg-Cl_2/L) removed 90% of the iodine in NOM-containing water (dissolved organic carbon concentration, 1.5 mg-C/L). Iodine removal in NOM-containing water increased with increasing chlorine dose up to 0.1 mg-Cl_2/L but decreased at chlorine doses of >1.0 mg-Cl_2/L. At a low chlorine dose, nonadsorbable iodide ion (I^-) was oxidized to adsorbable hypoiodous acid (HOI). When the chlorine dose was increased, some of the HOI reacted with NOM to form adsorbable organic iodine (organic-I). Increasing the chlorine dose further did not enhance iodine removal, owing to the formation of nonadsorbable iodate ion (IO_3^-). Co-existing Br^- depressed iodine removal, particularly in NOM-free water, because hypobromous acid (HOBr) formed and catalyzed the oxidation of HOI to IO_3^-. However, the effect of Br^- was small in the NOM-containing water because organic-I formed instead of IO_3^-. SPAC (median particle diameter, 0.62 μm) had a higher equilibrium adsorption capacity for organic-I than did conventional PAC (median diameter, 18.9 μm), but the capacities of PAC and SPAC for HOI were similar. The reason for the higher equilibrium adsorption capacity for organic-I was that organic-I was adsorbed principally on the exterior of the PAC particles and not inside the PAC particles, as indicated by direct visualization of the solid-phase iodine concentration profiles in PAC particles by field emission electron probe microanalysis. In contrast, HOI was adsorbed evenly throughout the entire PAC particle.

* *Corresponding author.* Tel./fax: +81 11 706 7280.
E-mail address: matsui@eng.hokudai.ac.jp (Y. Matsui).
http://dx.doi.org/10.1016/j.watres.2014.10.021
0043-1354/

1. Introduction

The Tohoku Earthquake on 11 March 2011 resulted in the release of large amounts of radioactive materials including iodine-131 (^{131}I) into the environment from the Fukushima Daiichi nuclear power plant. After the accident, ^{131}I was detected in drinking water in 15 out of the total 47 prefectures in Japan: the highest concentration in a village of Fukushima Prefecture was 1000 Bq/kg-water and the highest concentration in Tokyo Metropolitan was 200 Bq/kg-water (Ikemoto and Magara, 2011), which points to the importance of technologies for removal of radioactive substances during water purification processes. The radioactive iodine index levels for the restriction on drinking water intake in emergency by the Nuclear Safety Commission of Japan was 300 Bq/kg for the general public and 100 Bq/kg for infants (babies who take breast feeding or formula milk). The removal of radioactive iodine by 50–90 % was required.

The addition of powdered activated carbon (PAC) may be a feasible method for removal during conventional water treatment when accidents or incidents give rise to high levels of contamination in drinking water sources (Brown et al., 2008; Lettinga, 1972). However, the efficacy of ^{131}I removal by PAC was not sufficiently high. Kosaka et al. (2012) surveyed ^{131}I removal in water purification plants after the Fukushima accident and found that the removal percentages achieved by granular activated carbon and PAC were merely 30–40% or less. The authors also conducted laboratory tests and attained the removal efficiencies of 60–70% by PAC of the dosage 50 mg/L and the contact time 30 min after chlorination of the dosage 0.5–1 mg-Cl_2/L and reaction time 10 min.

Dissolved I (including ^{131}I) exists in various forms: molecular iodine (I_2), hypoiodite ion (IO^-), hypoiodous acid (HOI), iodide ion (I^-), iodate ion (IO_3^-), and organic iodine (organic-I). At neutral pH iodine can be present in the latter four forms (Bichsel and von Gunten, 2000a; Lettinga, 1972), while iodine is commonly found as I^-, IO_3^-, and organic-I in environmental waters (Davis et al., 2009; Gong and Zhang, 2013; Hansen et al., 2011). It has been reported that $^{131}I^-$ is poorly adsorbed by activated carbon (Ikeda and Tanaka, 1975; Lettinga, 1972). HOI is adsorbed on activated carbon to a greater extent than I^-: the adsorptive property of HOI is utilized in the iodine number, one of the most fundamental indicator widely used to characterize activated carbon as an adsorbent (AWWA, 1974). The removal of HOI is due to adsorption while that of chlorine is reductive reaction. Because HOI is formed by oxidation of I^-, the combination of chlorination and PAC adsorption could be effective for $^{131}I^-$ removal (Lettinga, 1972). However, $^{131}IO_3^-$, which is formed by oxidation of $HO^{131}I$, is reportedly not adsorbed by carbon (Lettinga, 1972). Therefore, chlorination of $^{131}I^-$ at a high chlorine dose, a long reaction time, or both would reduce the extent of adsorptive removal compared to that at a low dose and a short reaction time. During aqueous oxidation in the presence of natural organic matter (NOM), HOI reacts with NOM to form iodo-organic byproducts (Bichsel and von Gunten, 1999), which can be adsorbed by activated carbon (Summers et al., 1989). No systematic experimental study has been conducted to clarify how chlorination time, carbon type, and carbon dose affect iodine species distribution and, thus, iodine removal efficacy.

In this study, we systematically investigated the formation of iodine species by chlorination and their removal from water by activated carbon adsorption. The effects of chlorine dose, chlorination time, carbon particle size, NOM content, and co-existing bromide on iodine removal were evaluated to determine the optimum conditions for removal of radioactive iodine from water. We used ^{127}I rather than ^{131}I. But the adsorption behavior of ^{127}I is similar to that of ^{131}I. Therefore, information regarding ^{127}I removal can be expected to provide important insights for the removal of ^{131}I. The removal of iodide in water is also of great significance for controlling the formation of iodinated disinfection byproducts (Ding and Zhang, 2009; Plewa et al., 2004). Hereafter, we refer to ^{127}I simply as I (or iodine).

2. Materials and methods

2.1. Sample water

NOM-free water was prepared by adding inorganic ions to ultrapure water (Milli-Q Advantage, Millipore) so that the ionic composition was equal to that of water from Lake Hakucho, Hokkaido, Japan (Table S1, Supplementary Material) (Ando et al., 2010). NOM water was prepared by adding Suwannee River NOM (International Humic Substance Society) to the NOM-free water to bring the dissolved organic carbon (DOC) concentration to 1.5 mg-C/L unless otherwise noted. Potassium iodide was added to the NOM-free water and the NOM water, and then the pH was adjusted to 7.0 with HCl or NaOH; the iodine concentration was 10 μg-I/L, which is typical of natural surface waters. In the experiments on iodine removal in the presence of bromide ion (Br^-), KBr was also added, at concentrations ranging from 0 to 2000 μg-Br/L (Jones et al., 2011; Richardson et al., 2008). All chemicals used were regent grade (Wako Pure Chemical, Osaka, Japan).

2.2. Activated carbon

Two types of activated carbon were used. A commercially available, thermally activated wood-based PAC (median particle diameter, 18.9 μm) was obtained from Taiko-W, Futamura Chemical (Nagoya, Japan). A superfine PAC (SPAC, median particle diameter, 0.62 μm; Figures S1 and S2, Supplementary Material) was prepared by microgrinding the PAC with a bead mill (Metawater, Tokyo) (Ando et al., 2010). PAC and SPAC were stored as slurries in ultrapure water at 4 °C and used after dilution. The particle size distributions of PAC and SPAC were determined with a laser-light scattering instrument (Microtrac MT3300EXII, Nikkiso, Tokyo) following the addition of a dispersant (Triton X-100, Kanto Chemical, Tokyo; final concentration, 0.08 vol%) and ultrasonication.

2.3. Batch oxidation and adsorption tests

Sample water was treated with chlorine (in the form of sodium hypochlorite, Wako Pure Chemical) at concentrations of 0.01–50 mg-Cl_2/L for 1–60 min, and then activated carbon was added. After a carbon contact time of up to 30 min, the

suspension was filtered through a 0.2-μm membrane filter (DISMIC-25HP; Toyo Roshi Kaisha, Tokyo). In some experiments, water was treated first with carbon and then with chlorine. All experiments were conducted in the room temperature of 20 °C. Individual operation condition is described in figures. The concentration of free chlorine was determined by means of the *N,N*-diethyl-*p*-phenylenediamine colorimetric method (DR/4000U, Hach).

2.4. *Iodine fractionation*

The total iodine concentrations in sample waters were determined by means of inductively coupled plasma mass spectrometry (ICP-MS; 7700 series, Agilent Technologies) with tellurium as an internal standard (detection limit: 0.2 μg-I/L). Iodine fractionation was conducted by using total organic halide (TOX) analysis and ion-chromatography with post-column (IC-PC) derivatization (ICS-1100, PCM 520, UVD-510, Dionex) both for the samples treated with and without chlorine (Figures S3, Supplementary Material). The IC-PC was conducted according to the Dionex manual. KaBr/$NaNO_2$ mixture was used as PC derivatization reagent in order to form tri-iodide, which is detected using UV detector at 268 nm (detection limit: 0.1 μg-I/L).

Water samples with/without 10-min chlorination were treated with SPAC at a concentration of 100 mg/L for 30 min (these condition were determined for the complete removal of adsorbable iodine and bromine) and then filtered through a 0.2-μm PTFE membrane filter to obtain Sample A, which contained I^- and IO_3^- but did not contain HOI, as indicated by the results of a preliminary experiment (Supplementary Material, Section 1 and Figure S4). The total iodine concentration in Sample A was determined by ICP-MS, the IO_3^- concentration was determined for Sample A by IC-PC, and the I^- concentration was calculated for Sample A by subtracting the IO_3^- concentration from the total iodine concentration.

The organic-I concentrations were measured by means of TOX analysis, as follows (see Supplementary Material, Section 2 for details). After chlorination, NOM water was applied to a column of activated carbon. Then the column was washed with KNO_3 solution to remove any HOI bound to the carbon. The carbon packing was then removed from the column and heated in a muffle furnace, and the combustion gas was bubbled through Milli-Q water (the resulting solution was designated as Sample B). Any iodine in Sample B was regarded as organic-I (Tate et al., 1986). The iodine concentration in Sample B was determined by means of ICP-MS. The concentration of HOI was calculated by subtracting the iodine concentrations in Samples A and B from the initial iodine concentration, which was determined by ICP-MS. The percentages obtained by the fractionation method were verified by comparing them with the concentrations obtained by an alternative method (Supplementary Material, Section 3 and Figure S5) in which the concentration of HOI in the eluent from the activated carbon column used for TOX analysis was determined by ICP-MS.

2.5. *Bromine fractionation*

Bromine was fractionated in conjunction with iodine fractionation. The total bromine concentration and the bromate ion (BrO_3^-) concentration were determined by ICP-MS (detection limit: 5 μg-Br/L) and IC-PC (detection limit: 0.5 μg-Br/L), respectively (Figures S6, Supplementary Material). Because Br^- is not adsorbed by activated carbon whereas hypobromous acid (HOBr), BrO_3^-, and organic bromine (organic-Br) are adsorbed (Siddiqui et al., 1996), the concentration of Br^- was determined by means of ICP-MS for Sample A (the mechanism that HOBr is adsorbed but not reduced to Br^- by activated carbon was confirmed by the decrease of total bromine concentration determined by ICP-MS. Section 3.3). The organic-Br concentration was measured for Sample B by means of ICP-MS. The HOBr concentration was calculated by subtracting the sum of the concentrations of Br^-, BrO_3^-, and organic-Br from the total bromine concentration.

2.6. *Direct observation of iodine adsorbed on PAC particles*

To obtain PAC particles containing adsorbed HOI and adsorbed organic-I, we conducted batch adsorption experiments. After batch adsorption, PAC particles were removed, placed on a silicon wafer, and then cut. Iodine adsorbed on the cut PAC particles was directly observed by means of scanning electron microscopy and field emission electron probe microanalysis (FE-EPMA; JXA-8530F, JEOL). Details of these experiments are described in the Supplementary Material (Section 4 and Figures S7 and S8).

3. Results and discussion

3.1. *Iodine removal by activated carbon after chlorination*

Without prior chlorination, I^- in the NOM-free water was not removed by activated carbon treatment (Figure S9, Supplementary Material). No removal of I^- from NOM water was observed either. In contrast, when chlorine was added to the NOM-free water before activated carbon treatment, about 40% of the iodine was removed. After the chlorination, iodine in the NOM water was removed at a higher percentage (90%) by activated carbon treatment than in the NOM-free water. This removal percentage was similar but slightly higher than the DOC removal percentage (80%). The similar removal suggests that the formation of organic-I was responsible for the high iodine removal percentage in the presence of NOM. The slightly higher removal is possibly due to HOI removal.

We further studied the effect of NOM by varying the initial DOC concentration in the sample water. Even a DOC concentration as low as 0.5 mg-C/L drastically improved adsorptive removal of iodine by SPAC after chlorination (Panel A of Fig. 1). At a fixed SPAC dose of 100 mg/L, the residual iodine ratio decreased as the initial DOC concentration was increased from 0 to 3 mg-C/L, but the ratio increased as the DOC concentration was increased further from 3 to 10 mg-C/L. This increase in residual ratio was due to the insufficiency of the carbon dose; when the carbon dose was increased to >100 mg/L, the ratio continued to decrease with increasing DOC concentration above 3 mg-C/L (Fig. 1, Panel A, dashed line). The residual ratios indicated by the triangles in Panel A

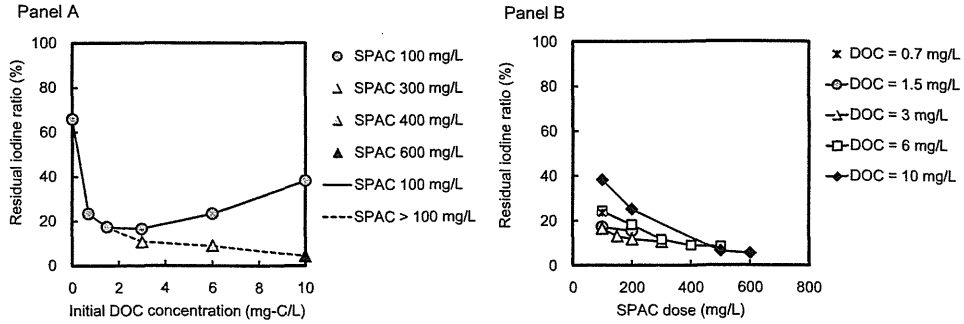

Fig. 1 – Effect of initial DOC concentration (left) and SPAC dose (right) on iodine removal from NOM water by chlorination followed by treatment with SPAC. Initial I^- concentration in sample water, 10 μg-I/L; chlorine dose, 1 mg-Cl_2/L; chlorination time, 10 min; carbon contact time, 30 min.

of Fig. 1 were achieved when a sufficient amount of SPAC was used; the amount that was sufficient was confirmed by testing various combinations of SPAC dose and DOC concentration (Fig. 1, Panel B). The data points indicated by the triangles can be considered to be the lowest residual iodine ratios attainable by adsorptive removal with SPAC. These results indicate that the percentage of iodine converted to adsorbable forms increased with increasing NOM concentration: at the DOC of 10 mg-C/L, 95% of I^- was converted to adsorbable forms.

3.2. *Chlorine-dose dependence and iodine fractionation analysis*

The results described in the previous section indicate that the iodine was converted to an adsorbable form by chlorination. Next we studied the effect of chlorine dose. For NOM-free water, a chlorine dose of approximately 0.1 mg-Cl_2/L was found to be optimal, yielding the lowest residual iodine ratio (Figure S10, Supplementary Material). A similar trend was observed for NOM water, although low residual iodine ratios were observed over a broader range of chlorine doses (0.1–1.0 mg-Cl_2/L). Iodine removal increased with increasing chlorine dose up to 0.1 mg-Cl_2/L but decreased at chlorine doses of >1.0 mg-Cl_2/L. Overall, the residual ratios were lower in the presence of NOM than in its absence.

To elucidate the mechanism of the dependence of iodine removal on chlorine dose, we conducted iodine fractionation. In NOM-free water (Fig. 2, Panel A), the production of HOI was highest at a chlorine dose of 0.05–0.1 mg-Cl_2/L, and production decreased as the chlorine dose was increased from 0.1 to 10 mg-Cl_2/L. Therefore, a moderate chlorine dose (0.05–0.1 mg-Cl_2/L) was most effective for the formation of HOI, which was adsorbed by activated carbon. At high chlorine doses (>0.1 mg-Cl_2/L), IO_3^- formed, and IO_3^- became the major species at chlorine doses of >1 mg-Cl_2/L. The percentages of IO_3^- fraction were almost similar but somewhat higher than those calculated by the reaction rate constants reported previously (Bichsel and von Gunten, 1999): the experimental percentages were 1.9, 38, and 100 while the calculated ones were 1.5, 14, and 88 at the chlorine doses of 0.1, 1 and 10 mg-Cl_2/L, respectively. The somewhat higher IO_3^- percentages might be due to the enhanced oxidation at very low iodine concentration in our experiments.

When the water contained NOM (DOC concentration, 1.5 mg-C/L), organic-I formed (Fig. 2, Panel B). The concentration of organic-I increased as the chlorine dose was

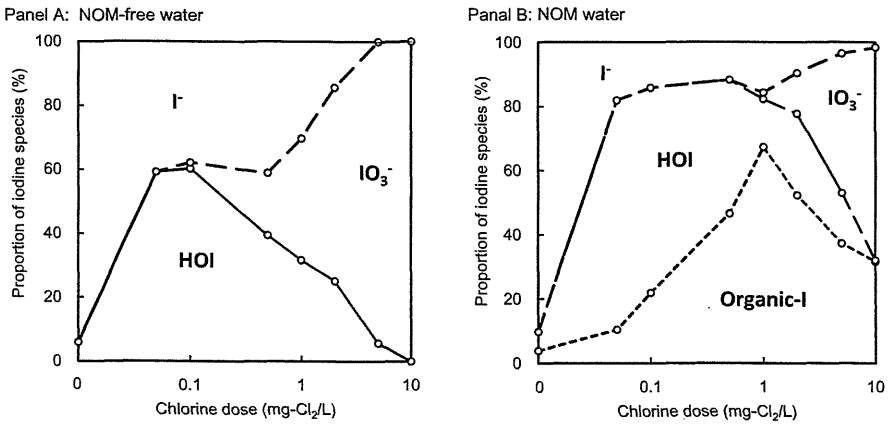

Fig. 2 – Proportions of iodine species in NOM-free water (left) and NOM water (right) as a function of chlorine dose. Chlorination time, 10 min; initial I^- concentration in sample water, 10 μg-I/L; initial DOC concentration in NOM water, 1.5 mg-C/L.

increased from 0.05 to 1 mg-Cl_2/L, and then it decreased. The latter finding is qualitatively in agreement with the results of studies of iodotrihalomethane formation, in which an increase in chlorine doses was found to lead to a decrease in the levels of iodinated organic byproducts and an increase in IO_3^- formation (Bichsel and von Gunten, 2000b; Hua et al., 2006). We found that organic-I was the major species at high chlorine doses (0.5–5 mg-Cl_2/L) and that HOI was the major species at low doses (0.05–0.5 mg-Cl_2/L). We inferred that at chlorine doses of >1.0 mg-Cl_2/L in the NOM-free water, HOI was promptly oxidized to IO_3^-, which was not adsorbed by activated carbon. However, in the NOM water at a high chlorine dose, the formation of organic-I prevented the formation of IO_3^-. The use of chlorine doses of 0.1–0.5 mg-Cl_2/L resulted in the formation of the highest amount of adsorbable iodine (HOI and organic-I) and thus to the highest iodine removal efficiency.

3.3. *Effect of co-existing Br^- on the removal of I^-*

Br^- have been shown to influence the formation of iodinated trihalomethane during water treatment by means of chlorination (Jones et al., 2012), and thus the presence of Br^- can be expected to have an impact on iodine oxidation by chlorination. As shown in Panel A of Fig. 3, the residual iodine ratio in the NOM-free water slightly increased as the Br^- concentration was increased from 0 to 10 μg-Br/L, and the increase in residual iodine ratio with increasing Br^- concentration was more rapid in the concentration range from 10 to 200 μg-Br/L. This result indicates that co-existing Br^- in the water inhibited iodine removal. In the NOM-free water, IO_3^- formation increased dramatically with increasing initial Br^- concentration in the range from 10 to 200 μg/L (Panel B of Fig. 3). In contrast, little IO_3^- was formed in the presence of Br^- in the NOM water. The effect of Br^- on iodine removal was largely attributable to enhanced formation of nonadsorbable IO_3^- in the presence of Br^-.

To further elucidate the effect of Br^- on the oxidation of I^- by chlorine, we conducted iodine and bromine fractionation. As shown in Panel A1 of Fig. 4, in NOM-free water containing Br^-, the proportion of HOI was the largest at a chlorine dose of 0.1 mg-Cl_2/L. IO_3^- formed at chlorine doses of >0.1 mg-Cl_2/L and became the major iodine species at chlorine doses of >1 mg-Cl_2/L. This result was similar to that observed in the absence of Br^- (Fig. 2, Panel A). However, the percentage of IO_3^- formation at chlorine doses of >0.1 mg-Cl_2/L (and particularly at a chlorine dose of ~1 mg-Cl_2/L) was higher in the presence of Br^- than in the absence of Br^-. At a chlorine dose of 1 mg-Cl_2/L, IO_3^- formation in the presence of Br^- was 1.7 times that in the absence of Br^-. Bromine fractionation revealed that in the NOM-free water, HOBr was formed at a chlorine dose of 0.05 mg-Cl_2/L, and the proportion of HOBr increased with increasing chlorine dose up to 2 mg-Cl_2/L (Fig. 4, Panel B1). This chlorine dose range roughly coincided with the range at which IO_3^- formation was higher in the presence of Br^- than in its absence. It was recently reported that increasing the Br^- concentration increases the oxidation of HOI to IO_3^- (Criquet et al., 2012), as a result of a bromide-catalyzed process where the following reaction sequence is proposed. HOBr is formed through the reaction of chlorine with Br^-. HOBr then oxidizes HOI to IO_3^- and thereby HOBr is reduced to Br^-. Our results confirm that Br^-/HOBr-catalyzed process: we found that when HOBr was formed by the oxidation of Br^- by chlorine, the oxidation of HOI to IO_3^- was enhanced.

In the NOM water, iodine removal was not greatly influenced by the presence of Br^- (Panel A of Fig. 3). However, the nature of the adsorbed iodine species differed in the absence and presence of Br^- (Fig. 2, Panel B; Fig. 4, Panel A2). More organic-I was formed at a chlorine dose of ~0.1 mg/L in the presence of Br^- than in its absence, while more IO_3^- was formed at chlorine doses >5 mg/L. The enhanced formation of organic-I may possibly be due to a reaction process similar to the Br^-/HOBr-catalyzed process of IO_3^- formation. As shown in panel B2 of Fig. 4, the proportion of HOBr was high at chlorine doses of >0.5 mg-Cl_2/L. However, at chlorine doses ranging from 0.05 to 0.1 mg-Cl_2/L, the proportion of HOBr was low. Nonetheless, a large amount of organic-I was formed at this low chlorine dose range. There is, however, a possibility that

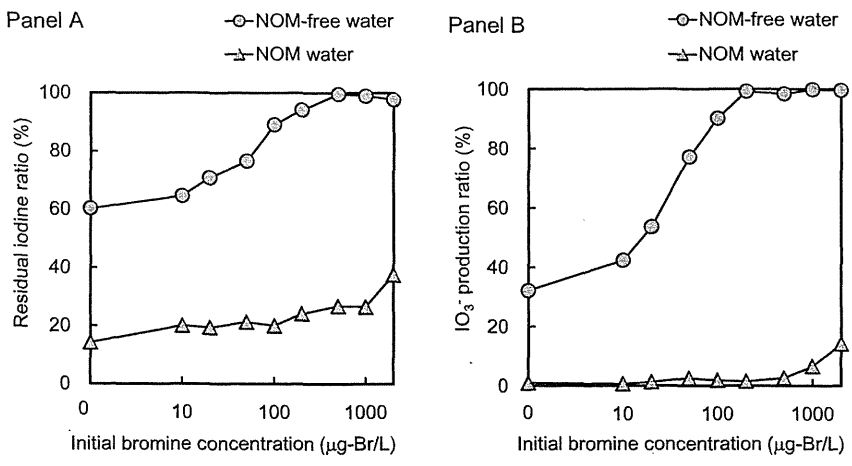

Fig. 3 – Effect of initial Br^- concentration on adsorptive removal of iodine (left) and IO_3^- production ratio (right). SPAC dose, 100 mg/L; initial I^- concentration in sample water, 10 μg-I/L; initial DOC concentration in NOM water, 1.5 mg-C/L; chlorine dose, 1.0 mg-Cl_2/L; chlorination time, 10 min; carbon contact time, 30 min.

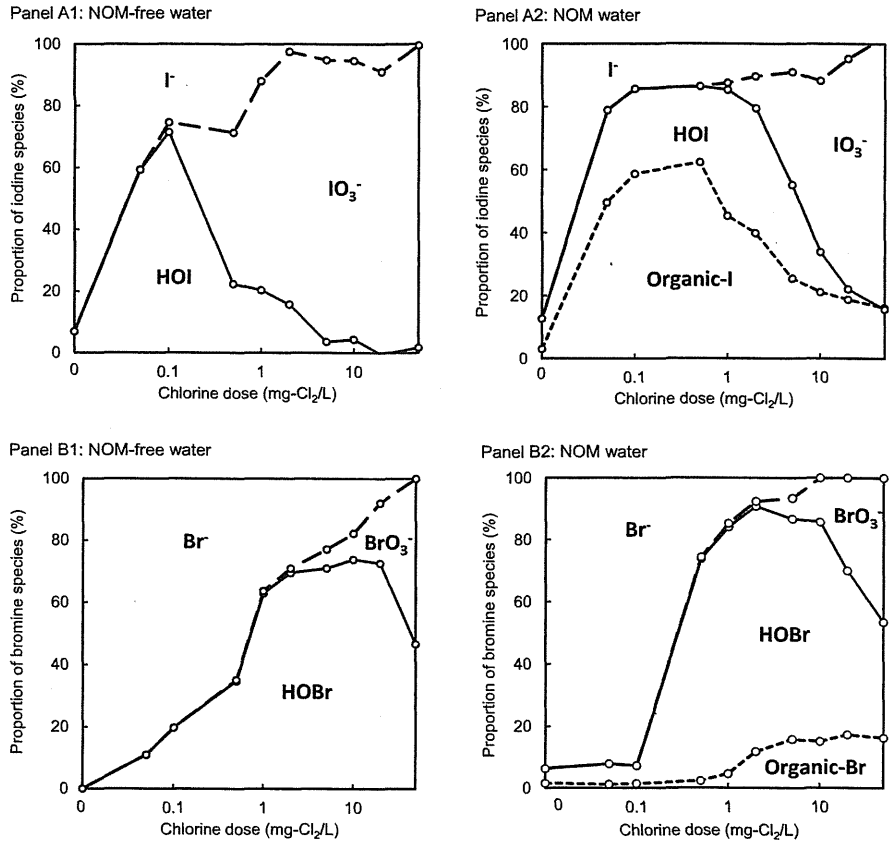

Fig. 4 – Proportions of iodine species (top) and bromine species (bottom) formed in the presence of Br^- as a function of chlorine dose. Chlorination time, 10 min; initial I^- concentration in sample water, 10 μg-I/L; initial Br^- concentration, 100 μg-Br/L; initial DOC concentration in NOM water, 1.5 mg-C/L.

HOBr had been once formed but it was converted back to Br^-. Without clear data of HOBr formation, it cannot be concluded that organic-I was formed through the Br–/HOBr-catalyzed process. Further study is granted for the mechanism of the enhanced formation of organic-I in the presence of bromide.

3.4. *Effects of chlorination and reaction sequence*

We also evaluated the effect of chlorination time (1–60 min) on the residual iodine ratio (Fig. 5). The lowest residual ratio was observed at the shortest chlorination time (1 min). This result suggests that the oxidation of I^- to HOI was fast and that the oxidation of HOI to IO_3^- occurred continuously as long as free chlorine was present in the water. The fast oxidation reaction of I^- to HOI and the following slow oxidation reaction of HOI to IO_3^- are in agreement with the reaction kinetics calculations with the rate constants reported previously (Bichsel and von Gunten, 1999; Criquet et al., 2012; Kumar et al., 1986): half life of I^- in the presence of HOCl of >1 mg-Cl_2/L is < 1 ms while that of HOI was <45 min. Therefore

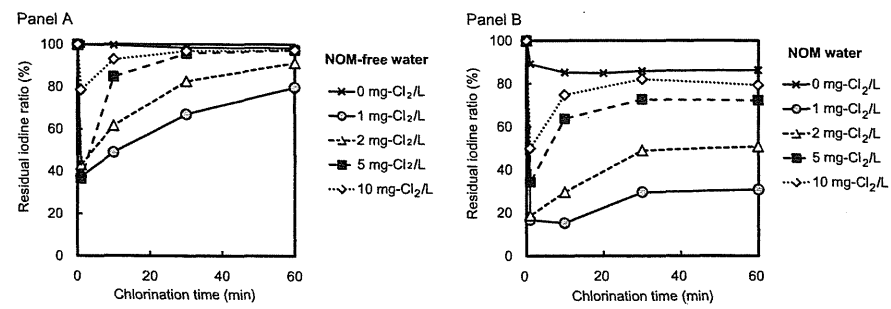

Fig. 5 – Effects of chlorination time and chlorine dose on iodine removal from NOM-free water (left) and NOM water (right). After chlorination, 100 mg/L of SPAC was added. Initial I^- concentration in sample water, 10 μg-I/L; initial DOC concentration in NOM water, 1.5 mg-C/L; carbon contact time, 30 min.

chlorination in the presence of carbon could enhance iodine removal if HOI adsorption occurred before HOI was oxidized to IO_3^-. To evaluate this possibility, we conducted two experiments: in one experiment (Case 1), water was chlorinated first and then activated carbon was added, whereas in the other experiment (Case 2), water was chlorinated after activated carbon was added.

In the NOM-free water (Fig. 6, panel A1), lower residual iodine ratios were obtained in Case 2 than in Case 1 at chlorine doses of >0.3 mg-Cl_2/L. Panel A2 of Fig. 6 shows IO_3^- formation ratio and residual chlorine ratios for the two experiments. In Case 2, the formation of IO_3^- was depressed compared to that in Case 1. The carbon consumed the chlorine so that the formation of IO_3^- by oxidation of HOI was suppressed. Therefore, after HOI formed, it was efficiently adsorbed by the carbon. At low chlorine doses (<0.2 mg-Cl_2/L), however, iodine removal was lower in Case 2 than in Case 1, owing to the consumption of chlorine by carbon before the chlorine could oxidize I^- to HOI.

We also compared the results for Cases 1 and 2 with NOM water. Although iodine removal was higher in Case 2 than in Case 1 at high chlorine doses (>5 mg-Cl_2/L; Fig. 6, panel B1), the difference between the two cases for the NOM water was not as clear as that for the NOM-free water. This result is reasonable because IO_3^- formation in the NOM water was depressed by the formation of organic-I, even in the absence of activated carbon; the IO_3^- formation was smaller in the presence of NOM than in the absence of NOM (compare Panels B2 and A2 of Fig. 6). The formation of IO_3^- was also somewhat depressed when the water was treated with activated carbon prior to chlorination (Case 2), and consequently iodine removal was slightly higher in Case 2 than in Case 1.

In Case 1, increasing the chlorine contact time depressed adsorptive removal of iodine because of the formation of IO_3^- from HOI (Fig. 5). However, a similar trend was not observed in Case 2, as shown in panels A1 and B1 of Fig. 7. The residual iodine ratios did not increase with increasing chlorine contact time; instead, the removal percentage increased until 10 min. This result also supports the reaction mechanism described above: soon after I^- was oxidized to HOI by chlorine, the HOI was adsorbed by the carbon, and only some of the HOI was further oxidized to IO_3^- in the presence of carbon. Meanwhile, activated carbon consumed the chlorine, which disappeared after 10 min (Fig. 7, panels A2 and B2). Therefore, iodine removal did not increase; rather, it reached a constant level after 10 min.

3.5. *Effect of carbon particle size on adsorption capacity*

The effect of carbon particle size on adsorption capacity was examined by calculating the adsorption isotherms from data obtained by batch adsorption experiments on prechlorinated sample water containing iodine. In the batch adsorption experiments, the water-phase iodine concentration did not change when the contact time was increased from 30 to 60 min (Figure S11, Supplementary Material). Therefore, we assumed that adsorption equilibrium was attained at a contact time of 30 min. The adsorption isotherms (Fig. 8) were obtained by mass balance after contact with PAC or SPAC, but note that the iodine in the water-phase might have consisted

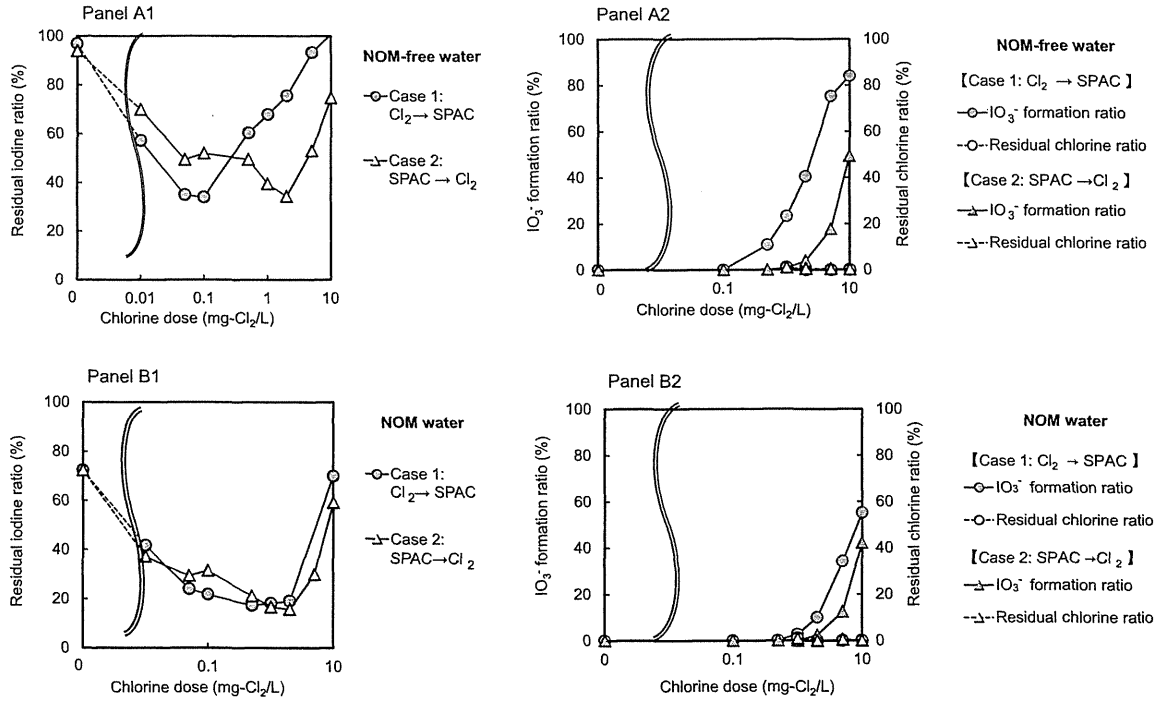

Fig. 6 – Effects of reaction sequence on residual iodine ratios (left) and IO_3^- formation ratios (right) in NOM-free water (top) and NOM water (bottom). Case 1: Chlorination followed by activated carbon treatment. Case 2: Chlorination preceded by activated carbon treatment. Initial I^- concentration in NOM water, 10 μg-I/L; SPAC dose, 100 mg/L; chlorination time, 10 min; carbon contact time for Case 1, 30 min; initial DOC concentration in NOM water, 1.5 mg-C/L.